

**SYNTHESIS AND CHARACTERIZATION
OF LIGNIN-CARBOHYDRATE BLOCK COPOLYMERS.**

by

Veronique DEMARET

Thesis submitted to the Faculty of the
Virginia Polytechnic Institute and State University
in partial fulfillment of the requirements for the degree of

MASTER OF SCIENCE

in

Chemical Engineering

APPROVED:

Wolfgang G. Glasser , Chairman

Garth L. Wilkes

Donald G. Baird

August, 1986

Blacksburg, Virginia

**SYNTHESIS AND CHARACTERIZATION
OF LIGNIN-CARBOHYDRATE BLOCK COPOLYMERS.**

by

Veronique DEMARET

Wolfgang G. Glasser , Chairman

(ABSTRACT)

Hydroxypropyl lignin derivative block (HPL) was reacted with low DP cellulose triacetate block (CTA). The synthesis of this block copolymer involves the following steps.

- Synthesis of an hydroxyl-terminated CTA oligomer through the depolymerization of high molecular weight cellulose triacetate under conditions that deacetylation is prevented.
- Reaction of this block with 2,4 toluene diisocyanate (TDI) to form an isocyanate-capped CTA prepolymer under conditions that chain extension is limited and a sufficient NCO equivalent/mole is achieved (ie: 1 or 2).
- Reaction in solution of this low DP CTA prepolymer with the HPL block.

Films were directly obtained by solution casting of the mixture and cured. The parameters of investigation were HPL, or CTA block content and size of CTA block. Morphological characteristics and thermal analysis were investigated as a function of these parameters. Analysis of the results showed that all the films were brittle. They exhibited single T_g values and were crystalline even for short size cellulose blocks. Network structure was not the predominant factor influencing the properties as was expected from the multi-hydroxyl functionality of the HPL component but rather the crystalline character observed in the copolymers at all compositions.

Acknowledgements

I especially acknowledge the support and the confidence of Rafael JORDA and the assistance of Dr CONGER and Dr WILKES, without whom I would never have studied in this university.

I would like to thank Dr GLASSER, my major professor, who gave me the opportunity to study in his laboratories. I do greatly appreciate his help and patience which allowed me to perform this work in the best conditions.

I wish to thank Charlotte BARNETT whose help has been so valuable and my committee members, Dr WILKES and Dr BAIRD for their interest in this research.

Table of Contents

1.0 INTRODUCTION	1
1.1 LIGNIN REVIEW	1
1.2 CELLULOSE REVIEW	4
1.3 OBJECTIVES AND JUSTIFICATION	7
2.0 MATERIALS AND METHODS	11
2.1 MATERIALS	11
2.2 METHODS	12
2.2.1 MATERIAL ANALYSIS	12
2.2.1.1 Determination of acetyl content of parent CTA	12
2.2.1.2 Determination of hydroxyl content of parent CTA and HPL	13
2.2.1.3 Average molecular weight of parent CTA and HPL	14
2.2.1.4 Thermal analysis	15
2.2.2 SAMPLE PREPARATION	16
2.2.2.1 CTA oligomer synthesis, (Parent CTA depolymerization).	16
2.2.2.2 CTA prepolymer synthesis, (TDI capping of CTA oligomer)	17
2.2.2.3 Copolymer synthesis	18
3.0 RESULTS AND DISCUSSION	20
3.1 BLOCK COPOLYMER SYNTHESIS	20
3.1.1 CELLULOSE ACETATE COMPONENT	20
3.1.1.1 Parent CTA (starting material)	20
3.1.1.2 CTA oligomers	23

3.1.1.3 CTA prepolymers (TDI-capped CTA oligomers)	24
3.1.2 HYDROXY PROPYL LIGNIN COMPONENT	28
3.1.3 BLOCK COPOLYMERIZATION	28
3.2 BLOCK COPOLYMER PROPERTIES	30
4.0 CONCLUSIONS	39
5.0 FIGURES	41
6.0 TABLES	63
7.0 APPENDIXES	69
BIBLIOGRAPHY	71
VITA	75

LIST OF FIGURES

	Page
1 - Schematic representation of a softwood lignin structure by Freudenberg.....	41
2 - Schematic computer simulation structure for hardwood lignin by Glasser.....	42
3 - Schematic representation of a hydroxypropyl (organosolv) lignin derivative structure.....	43
4A - Cellulose structure.....	44
4B - The unit cell of native cellulose.....	44
5A - Synthesis route for cellulose triacetate.....	45
5B - Synthesis route for the depolymerization of cellulose triacetate (CTA).....	45
6 - Synthesis route for phenyl-monoisocyanate capped CTA.....	46
7 - Infrared spectrum of Parent CTA and phenyl- monoisocyanate capped CTA.....	47
8A - Relationship between carbanilate content and ultraviolet absorbance of phenyl-monoisocyanate capped CTA.....	48
8B - Relationship between carbanilate content and hydroxyl content of CTA.....	48
9 - Ultraviolet spectrum of phenyl-monoisocyanate capped CTA.....	49
10 - Relative viscosity versus concentration for Parent CTA (DP = 355).....	50
11 - DSC thermogram of Parent CTA.....	51

12 - DMTA curve of Parent CTA.....	52
13 - Relationship between degree of polymerization (DP) and time of depolymerization of Parent CTA (DP=355).....	53
14 - Relationship between the hydroxyl functionality of the CTA oligomers and the water added at the end of the depolymerization reaction of CTA (DP=355).....	54
15 - Infrared Spectrum of CTA oligomer of DP=20 (C20) and TDI capped oligomer C20 (TC20).....	55
16 - DSC thermogram of TDI capped oligomer C20 (TC20) and TDI capped oligomer C32 (TC32).....	56
17 - VPO curve for HPL.....	57
18 - DSC thermogram of HPL, P4608 (copolymer from TC46), P2008 (copolymer from TC20), P3210 (copolymer from TC32).....	58
19 - Relationship between HPL content and T_g	59
20 - Relationship between heat of fusion and cellulose content.....	60
21 - Sol fraction versus polysaccharide block content.....	61
22 - WAXS results of the copolymers.....	62

LIST OF TABLES

	Page
I - Characteristics of CTA block component.....	63
II - Infrared assignment bands of C20 and TC20....	64
III - DSC results of prepolymers.....	65
IV - Formulation parameters of the copolymers.....	66
V - Thermal characteristics from DSC experiments.	67
VI - Results from the swelling studies.....	68

APPENDIXES

I - Summary of the analytical results on the starting materials.....	69
II - Benzil calibration for VPO experiments.....	70

1.0 INTRODUCTION

1.1 LIGNIN REVIEW

Among natural polymers, lignin is second in abundance to cellulose. As aromatic and crosslinked three dimensional network polymer, it is a component of plants and wood providing structural support and resistance to mechanical and biological degradation. From a technological point of view, the chemistry of lignin degrading reactions lies at the base of a huge world-wide industry which chemically converts wood and other plant materials into cellulosic pulps for the manufacture of paper and other products. Whatever process is employed for this purpose, solubilized, degraded lignin derivatives are by products and are available in millions of tons. Even in the recent past, the lignin component has largely constituted a wasted by product often ending up as a contaminant of streams, rivers and lakes. One must recognize that the wood pulping industries have been conscious of the need for keeping this by product lignin out of the environment.

From that, a great motivation has arisen in terms of research on lignin utilization. As aromatic material with phenolic and alcoholic functional groups, lignin can be halogenated, nitrated, alkylated, hydrogenated and sulfonated. Most of these reactions

which cause degradation and substitution as well as solubilization in common organic solvents, have been well studied in the expectation of producing useful products.

For the last years, the molecular structure of lignin has been studied and characterized (1 - 8). Researchers had the goal to define a chemical formula as done for all typical organic compounds. This formula has changed over the years and different formulations were proposed such as Braun's 1948 (9), Erdtman's 1949 (10) and Alder's 1956 (11, 12) formulation for lignin. In 1968, Freudenberg (3, 4) proposed a lignin structure in which the major components were guaiacyl propane subunits with 25% of p-hydroxy phenyl propane and 5% of syringyl propane units. This structure is shown in Fig.1. This schematic diagram proposed by Freudenberg has emerged from a knowledge of the intermediate precursors of lignin biosynthesis together with analytical data from lignin degradations. Nowadays, it can be assumed that the chemistry, formulation and transformation of lignin is well defined (13). Later, by means of computer techniques, a statistical lignin structure was developed for both hardwood and softwood by Glasser (8). The hardwood structure is shown in Fig.2.

Recently, derivatized lignin has become a compound for use in engineering plastics and other polymeric materials (ie: polyurethanes). Lignin, from its structural design, can be considered as a high impact strength, thermally resistant thermoset polymer. Most of the time it is associated in nature with crystalline cellulosic fibers, and the separation of lignin and carbohydrates remains incomplete.

Lignin has the potential of becoming an important compound for the polyurethane industry (14-21). This can be attributed to the reactivity of the hydroxyl groups with regard to the isocyanate groups. Lignin has been used as an agent for reinforcing elastomeric rubbers, polyethers and polyalkylene glycol based materials. It has been demonstrated that the final properties of those materials can find interesting applications in the field of adhesives, fibers, elastomers, foams and coatings. Its utilization

lies in its polydispersity and its multi hydroxyl functionality. If one wants to use lignin as a polyol compound in linear polyurethanes (22), a more uniformly functional derivative must be obtained. In this goal, lignin can be modified with propylene oxide. This converts phenolic into aliphatic hydroxyls. A representative structural scheme of a hydroxypropyl organosolv lignin (HPL) is shown in Fig.3. It must be noted in the formula that the chain extension parameter, (n) approaches zero for normal HPL preparation.

It has already been observed that the chemical modification of lignin by oxyalkylation improves its flexibility and uniforms its functionality (23). Moreover, polymers derived from this modified lignin are known to give compounds having low glass transition temperatures and networks having low rigidity. Therefore, the utilization of lignin is a new route in the plastics field, and engineered polyurethane copolymers are one example.

Recently, the field of engineered plastics from lignin has been advanced by reacting hydroxypropyl lignin with isocyanates only (11) and with polyethylene glycol or polybutadiene glycol with diisocyanates (24, 25, 26) simultaneously. In those studies the thermal and mechanical properties, and the effect of the crosslink density on properties (27), have been investigated as a function of lignin content. It was reported that the material characteristics can be controlled to engineer new materials having suitable applications for specific end uses.

Following the approach described in those recent papers, the goal of the present research was to study the replacement of the second glycol component by cellulose acetate having a diol functionality. Therefore, it becomes necessary to review a few concepts related to cellulose as a component in polymeric materials. This is presented in the following section.

1.2 CELLULOSE REVIEW

Cellulose is nature's most abundant organic polymeric material. For many years, cellulose chemistry has been the subject of much research, and a definite emphasis has been placed on chemical and biomedical degradation. The utilization of cellulose and its derivatives continues to offer opportunities in the plastics industry (28, 29).

The chemical and supermolecular structure of cellulose has been well defined (28, 29). Several single crystal studies and analytical techniques have proposed that cellulose is a highly crystalline linear, rod like molecule that has local conformations made of two and three fold helices. Its structure and molecular arrangement in space are shown in Fig.4A and 4B. In Fig.4B, it can be observed that chains in alternate plane are anti-parallel (ie: if the anydroglucose units in the front and rear planes of the cube have their N^o1 carbons pointing down, then in the next plane between them, the N^o1 carbon points up).

Cellulose is isolated for use in the paper and textile industry, and it is also used as a filler and biomatrix support for biodegradable polymers. Since 1960, a new class of materials called "graft copolymers" began to develop. Those materials were produced by activation of a reactive site (ie: OH bond) on cellulose, causing a second polymer to form.

The use of cellulose derivatives as linear, semi- crystalline, hydroxyl-functional polymers represents a wide range of achievements in terms of industrial innovations (30,31) (ie: graft copolymerization of carboxymethyl- cellulose with styrene, and other polysaccharides with acrylonitrile or vinylacetate). The manufacturing techniques of

those polymers have been largely correlated to the treatment of linear synthetic polymers.

Among the wide variety of cellulose derivatives the following compounds can be cited: cellulose nitrate, acetate and other esters, ether and xanthate. All those derivatives are produced by modification of the hydroxyl groups on cellulose. The principal derivative in large scale production is cellulose acetate with a variable degree of substitution. Even substituted by acetyl groups, cellulose remains crystalline and the acetate substitutes can take a predictable orientation with respect to the glucose unit. However, complete acetylation of cellulose has never been achieved. Some hydroxyl functionality always remains on the cellulosic chain because of its low accessibility.

Cellulose acetate compounds can find many different applications, mainly because of their solubility in organic solvents compared to unmodified cellulose which is extremely difficult to dissolve in most of the common organic solvents. Among those applications are: fibers, films for the packaging and photographic industry, membranes for dialysis and water purification and coatings. Cellulose acetate is prepared by reacting highly purified cellulose with acetic anhydride, utilizing acetic acid as solvent and sulfuric acid as catalyst (32, 33). The synthesis route is represented in Fig.5A.

The synthesis of graft and block copolymers from cellulose acetate has been importantly advanced since 1973 by Stannett and Gilbert (34-40). In order to prepare block copolymers, cellulose triacetate (CTA) having only hydroxyl end groups needed to be synthesized. Work by Steinmann (41), showed that this could be accomplished, and that optimum conditions of high molecular weight CTA depolymerization exist which produce hydroxyl-terminated CTA oligomers during cleavage. Difunctional CTA blocks were diisocyanate-capped and reacted with other hydroxyl-terminated polymers. The second block component near cellulose consisted mainly in polyesters, polyethers or in polypropylene glycols (36, 37, 38, 41).

By this method Steinmann (41), succeeded in preparing elastomeric fibers from cellulose block copolymers. Stannett and Gilbert oriented their work toward improving the synthetic methods (38, 39) and their main purpose was to study the biodegradability and the water sorption properties of those copolymers. They studied the properties as a function of the size of the cellulosic block and their crystallization behavior. The degree of crystallinity of the cellulosic block was influencing the ability of the copolymer to absorb water, even if the crystallinity was low compared to that of normal cellulose (37).

For the synthesis of block copolymers, the problem was to achieve hydroxyl-terminated cellulose triacetate "macromers" because otherwise parallel reactions such as grafting or crosslinking were occurring (34, 36, 39, 40). Two consecutive acetylations of the carbohydrates seemed to give good results (39, 40) in terms of degree of acetyl substitution, and network formation during copolymer synthesis was almost prevented. Other workers (42, 43), tried to improve reaction conditions such that crosslinking through the second hydroxyl group in cellobiose was avoided. However, with significant improvements, this was not completely successful and chain branching or grafting occurred. This is the reason why in all the synthetic methods described, only the non-cellulosic block (ie: diol polyether) was end capped with a diisocyanate without isolation, and this was subsequently reacted with carbohydrate oligomers. The procedure of copolymers synthesis, therefore, involved always one step only.

In spite of some difficulties in achieving such copolymers, it is possible to synthesize block copolymers from cellulose acetate not only with diol polymers but also with styrene and chloroprene (44), diisocyanates alone (45), and with block types leading to star-like block copolymers (46).

This literature review illustrates that block copolymers from two natural polymers having greatly different chemical properties, hydroxypropyl lignin and cellulose acetate, can be expected to produce materials with unique properties.

1.3 OBJECTIVES AND JUSTIFICATION

Block copolymers have gained considerable interest in recent years because of their many unique properties. A review of the whole field has been published in 1973 (47). It is with the development of polyurethanes that block copolymers achieved pre-eminence. The architecture and location of the different blocks within the material were found to affect strongly the properties such as elastomeric behavior, melt rheology and toughness in rigid materials. Those properties are mainly due to the coexistence of a "hard" segment (T_m and T_g are above room temperature), and a "soft" segment (T_g is below room temperature). The hard block acts as reinforcing site within the material, while the soft block confers the material its elastomeric nature. The behavior of block copolymers has been well described in a recent paper (48).

As cited in the lignin review, propylene oxide-modified lignin has been used as amorphous hard segment in the synthesis of copolymers, and cellulose acetate has independently been employed as semi-crystalline hard segment of polyurethane block copolymers. However, recent research (49) has illustrated that propylene oxide chain extension (ie: n rising to values above 1 or 2, Fig.3) on HPL produces a lignin derivative with T_g declining to values as low as -40°C . Thus it is possible to engineer lignin as a soft segment component as well. It is expected that a lignin derivative (block A)-cellulose derivative (block B) block copolymer would display thermal and mechanical

properties resembling similar types of materials, and obeying similar rules. The purpose of this study was, therefore, to synthesize a series of lignin-carbohydrate block copolymers in which the cellulose derivative block dimensions were varied.

The synthetic route involves a two step prepolymer synthesis. The first step is the preparation of a cellulose triacetate block having two hydroxyl end groups and a low degree of polymerization (ie: CTA oligomer). In the second step, preventing chain extension, this block is to be reacted with toluene diisocyanate (TDI). After isolation and characterization, the prepolymer (ie: TDI-capped CTA oligomer) is to be reacted with hydroxypropyl lignin (HPL) to form the block copolymer. The prepolymer route is a method commonly employed in polyurethane synthesis. It produces better organized blocks than the one step method in which the two diol compounds and the diisocyanate are mixed together simultaneously.

Cellulose blocks with low degrees of polymerization can be synthesized by two ways (41). The first involves sulfuric acid and water, and the second is based on 1,3 dioxolane, boron trifluoride etherate (as catalyst) in a mixture of ethylene chloride-methylene chloride and water. Steinmann (41) has demonstrated that the first method, even though it requires shorter reaction times, causes deacetylation and hydrolysis of acetyl groups. This results in blocks having higher hydroxyl content. But since the present research emphasizes the use of hydroxyl-terminated cellulose triacetate, there is a need to avoid deacetylation and to keep the hydroxyl content as low as possible. Therefore, the second method was selected even though it has other weaknesses such as longer reaction times of depolymerization. However, this method is more promising and acetyl migration, redistribution and repolymerization are minimized in this system. The synthesis route of low DP CTA oligomers is shown in Fig.5B.

Optimum conditions for the isocyanate end capping had to be defined. Cellulose acetate had previously been reacted with such monoisocyanates as phenylisocyanate.

Ghatge (50) used this procedure to study cellulose acetate membranes for desalination. His experimental procedure involved the reaction of a solution of cellulose acetate in pyridine with phenylisocyanate. After refluxing the mixture for 4 hours the product was isolated by precipitation in ethyl alcohol and characterized. This method lends itself for adoption to the use of diisocyanates instead of a monoisocyanate. Following Ghatge's method will permit the condensation of hydroxyl groups with one isocyanate group leaving the other isocyanate group free for further reaction with the lignin derivative block.

The choice of TDI as diisocyanate can be explained by two facts (51-53). After the reaction of the para-NCO group with an alcohol, the ortho-NCO group becomes ten times less reactive than initially, but increasing the temperature will reduce this difference in reactivity. It is then expected that at low temperature the condensation of the OH group with the para-NCO group of TDI will be favored. The second fact is that TDI based reactions are largely free from chain extension by comparison with other diisocyanates (53). Consequently, the molecular weight of the prepolymer remains very close to that of the initial oligomer, which constitutes one of the study parameters of this work.

Rahman (52) has prepared isocyanate terminated polyethylene oxide (PEO) with TDI as a first step for polyurethanes block copolymer synthesis. In this work the capping reaction is carried out in argon where TDI and PEO are stirred in benzene at 25°C for one hour with or without the presence of a catalyst (dibutyltin-dilaurate). The observations made are that when using the catalyst, the selectivity between the two NCO group decreases and more chain extension occurs. This is not in fact surprising since the purpose of the catalyst is to activate the reaction. But these authors also succeed in synthesizing NCO end capped PEO without chain extension. Therefore, this method even though modified, was used for the work with cellulose triacetate. Unlike PEO,

CTA does have some OH functionality within the backbone and not only at the end. No other methods from the literature were available, and even if shortcomings exist, they are at least minimized by the method selected.

This previous study suggests the following as an appropriate experimental procedure for synthesizing isocyanate-terminated cellulose. Pyridine was chosen as the solvent because it dissolves well cellulose acetate and it had already been used for the reaction with isocyanate (50). Moreover, pyridine is a mild catalyst for TDI based reactions compared to dibutyltin-dilaurate. The choice to work with a catalyst is based on that hydroxyl groups on cellulose are less accessible than those of PEO so that the reaction needs to be slightly activated. In addition to that, activation was also increased by working at higher temperatures than those stated by Rahman (51). The complete experimental procedure is described in the following section.

The copolymers were obtained by mixing the isolated prepolymer (TDI-capped CTA oligomer) and HPL in the presence of the catalyst. Films were directly obtained by casting the mixture from solution. This procedure has largely been employed in the synthesis of polyurethane films from lignin (25,26). The properties of the copolymers were studied as a function of two variables:

- HPL or cellulose weight fraction.
- Size or DP of the cellulose block.

Even though it is important to define structure-property relationships, emphasis must be given to the synthetic achievement of such new materials because this is a new way to link lignin and carbohydrates, and those materials can be expected to produce interesting results in terms of the understanding of wood structure.

2.0 MATERIALS AND METHODS

2.1 MATERIALS

Cellulose triacetate: (Parent CTA), supplied by Eastman Kodack Company (Rochester NY).

Organosolv Lignin: Organosolv (aqueous ethanol) lignin from mixed hardwoods was supplied by the Biological Energy Corporation of Valley Forge, PA.

Hydroxypropyl Lignin (HPL): Obtained from reaction of propylene oxide with organosolv lignin. Details on the procedures employed and of the characteristics have been reported elsewhere (54, 55, 56, 23).

Diisocyanate: 2,4 toluene diisocyanate (TDI), supplied by Eastman Company.

Catalyst: Dibutyltin-dilaurate, supplied by Union Carbide.

2.2 METHODS

2.2.1 MATERIAL ANALYSIS

Degree of acetylation, hydroxyl content, degree of polymerization, average molecular weight and thermal behavior of the initial materials were determined by the following methods.

2.2.1.1 Determination of acetyl content of parent CTA

The method was taken from "Methods in Carbohydrate Chemistry" (57) and slightly modified. Two samples and a control were prepared. For each sample, 1 g of CTA was dissolved in 75% ethanol and heated for 30 min at 50-60°C. Then, 50 cc of methylene chloride were added to improve the solubility. The flasks were left standing for one week, after which 40 cc of sodium hydroxide (0.5N) were added. Then, the excess alkali was titrated with HCl (0.486N) using phenolphthaleine as indicator. The percentage of acetyl content, Z, and acetic acid content, AA, were calculated according to the following equations :

$$Z = [(A - B)Nb - (C - D)Na] \times 4.3 / W \quad [1]$$

$$AA = Z \times 1.395$$

where:

A(B) = ml of NaOH added to the sample (control)

C(D) = ml of HCl added to the sample (control)

Nb = normality of NaOH

Na = normality of HCl

W = weight of the sample (grams)

The degree of acetyl group substitution or number of acetyl groups per anhydro-D-glucose unit of cellulose, n , can be calculated from the acetyl content as follow : If Mu is the molecular weight of the repeat unit of cellulose triacetate, the chemical formula of the repeat unit can be written as $C_6H_7O_5[COCH_3]_nH_{(3-n)}$ and $Mu = 162 + 42n$. If Z is the percentage of acetyl in CTA as expressed by Eq.1, it follows that:

$$n = (Z \times Mu) / (43 \times 1000)$$

$$n = Z \times (162 + 42n) / 4300$$

$$(4300 \times n) = (162 Z + 42 n Z)$$

$$(4300 - 42 Z) n = 162 Z$$

$$n = (3.86 \times Z) / (102.4 - Z) \quad [2]$$

2.2.1.2 Determination of hydroxyl content of parent CTA and HPL

For CTA, the hydroxyl content was determined using the carbanilation method (58,59). This method consists of reacting CTA with phenyl-mono isocyanate and then to determine the carbanilate content of the final product by ultra violet absorption. The synthesis route is shown in Fig.6.

The method of Malm (58) was modified; another solvent of precipitation was used to improve the isolation technique. A solution of 10 g/cc of CTA in pyridine was

poured into a closed vial. The solution was stirred at room temperature until it dissolved well and 0.5 cc of phenyl isocyanate were added. The mixture was stirred for 2 hours in a 120°C oil bath, cooled, precipitated and thoroughly washed with anhydrous ether. The white powder obtained was dried in a P₂O₅ atmosphere under vacuum at room temperature. The end of the reaction was verified by Infrared Spectroscopy.

Analysis: The ultraviolet analysis was made on a solution of 0.1% of the carbanilate in methylene chloride / methanol (9/1 w) (ie: 0.1231g in 100cc of CH₂Cl₂ / MeOH). The absorbance, A, was measured at 280 nm. From this, the carbanilate content, C, was obtained by multiplying the absorbance by 17.1. The total hydroxyl content, T_{OH}, was obtained from the following formula:

$$T_{OH} = (14.3 \times C) / (100 - C) \quad [3]$$

For HPL, the hydroxyl content has been determined by a standard procedure where the residual acetic acid was back titrated by NaOH after the reaction of HPL with acetic anhydride (23).

2.2.1.3 Average molecular weight of parent CTA and HPL

The average molecular weights, \bar{M}_n , were determined by capillary viscosimetric measurements for CTA in CH₂Cl₂ / MeOH (9/1 w) at 25°C (60) and vapor pressure osmometry (VPO) for HPL in EtCl₂ at 45°C. Measurements of viscosimetry were made using a capillary viscosimeter. Different concentrations (expressed in g/dl) were prepared and the time of elution was measured for each concentration and the pure solvent. VPO measurements were made using a Knauer Vapor Phase Osmometer equipped with

universal thermistor probes. Calibration was obtained with benzil. Solutions ranging from 20 to 80 g/(kg of solvent) were used and the equilibrium time was identical than that of the calibration (ie: 3 minutes). Measurement conditions for the lignin were identical than those used in the calibration.

2.2.1.4 Thermal analysis

Heat capacity changes with temperature were measured by Differential Scanning Calorimetry (DSC). The measurement were performed on a Perkin Elmer DSC-4 system equipped with a Thermal Analysis Data Station using the scanning auto zero accessory. Five to 10 mg of material were tested under nitrogen atmosphere at 20°C/min. The glass transition temperatures, T_g , were defined as one-half the change in heat capacity that occurs over the transition of the second scan. The CTA sample was treated as follows. It was heated to the melting point at 100°C/min, quenched to 30°C at 200°C/min and heated at 20°C/min. The HPL sample was heated to 160°C at 100°C/min quenched at 200°C/min and heated at 20°C/min.

Temperature dependence modulus ($\log E'$) and damping factor ($\tan \delta$) of parent CTA was measured using Dynamic Mechanical Thermal Analysis (DMTA). DMTA was performed on a Polymer Laboratories' Dynamic Mechanical Thermal Analyzer interfaced to a Hewlett-Packard 9816 microcomputer. Temperature scans were performed at a heating rate of 4°C/min, a frequency of 1 Hz, and a strain level of 1%. Sample geometry involved a single cantilever beam.

2.2.2 SAMPLE PREPARATION

Block copolymers from HPL and CTA oligomer (low DP CTA) were prepared by the following methods.

2.2.2.1 CTA oligomer synthesis, (*Parent CTA depolymerization*).

Following the method of Steinmann (41), the parent CTA sample (20 g) was dissolved in a mixture of 300 cc of ethylene chloride and 20 cc of methylene chloride. Then, the system was dried by distillation until 20 cc of distillate was removed. When the temperature had dropped to 75°C, 20 g (19 cc) of 1,3 dioxolane were added followed by the addition of 0.5 cc of BF₃ (40% etherate). The mixture was stirred for different periods (to achieve variable molecular weights) at 75°C. At the end water (variable volumes) and 0.6 cc of triethylamine were added to neutralize the catalyst. If the solution was too viscous, it was diluted with the solvent. After filtration, the solvent was evaporated and the yellowish powder was soaked in 2-propanol for several hours and further digested by boiling in water for 2 hours. Finally, the white powder was isolated and dried in an oven at 100°C. The hydroxyl content of each oligomers was determined from Eq.3 by the carbanilation method in the same way as already described for the parent CTA. The number of OH groups or OH equivalent per mole of CTA oligomer (nOH/mole) and per monosaccharidic repeat unit (nOH/unit) were calculated according to the following equations:

$$\text{nOH/mole} = (T_{\text{OH}} \times \overline{M}_n) / 1700 \quad [4]$$

$$\text{nOH/unit} = (T_{\text{OH}} \times \text{Mu}) / 1700 \quad [5]$$

where, T_{OH} , is the hydroxyl content calculated from Eq.3, \bar{M}_n , is the molecular weight of the CTA oligomer and, μ is the molecular weight of a repeat unit (ie: anhydro-D-glucose unit).

The molecular weight, \bar{M}_n , of the depolymerized fractions (CTA oligomer) was measured either by VPO for lowest molecular weights or viscosity analysis for higher molecular weights under the same conditions as for the parent CTA.

2.2.2.2 CTA prepolymer synthesis, (TDI capping of CTA oligomer)

A solution of 0.1 g/cc of cellulose acetate oligomer in pyridine was prepared and stirred at room temperature under a nitrogen atmosphere. To this, TDI was added under nitrogen and the temperature was raised to a predetermined value and stirred for a variable period. At the end, the mixture was precipitated into anhydrous ether. During that step, the excess TDI and the pyridine remain dissolved in ether. This white precipitate was thoroughly washed with ether and dried under vacuum with P_2O_5 at room temperature. The reaction was analyzed by Infrared Spectroscopy. Then, the NCO content was determined by the procedure described below and the molecular weight by VPO. DSC experiments were also performed on the samples.

Analysis: The NCO content was measured by a known procedure (61). The TDI capped oligomer, 0.1 g, was dissolved in 5 cc of toluene. This mixture was allowed to stir vigorously at room temperature until all was dissolved. Addition of $EtCl_2$ helped the dissolution. Then, 5 cc of N-butylamine (around 0.1 N) were added and the mixture was allowed to stir for at least 15 minutes at room temperature. Then, 20 cc of 2-propanol were added to maintain two phase-miscibility and the excess amine was titrated by HCl

(0.1 N) using blue bromophenol as indicator. A control was run and titrated in the same way. The NCO content, T_{NCO} , was calculated according to :

$$T_{\text{NCO}} = (V_b - V_s) \times N \times 4.202 / W \quad [6]$$

where:

V_b (V_s) = volume (cc) of HCl added to the control (sample).

N = normality of HCl.

W = weight of the sample (grams).

Molecular weight was measured by VPO, and knowing the NCO content, the number of NCO groups or NCO equivalent per mole of prepolymer, $n\text{NCO}/\text{mole}$, was calculated as:

$$n\text{NCO}/\text{mole} = (T_{\text{NCO}} \times \overline{M}_n) / 4200 \quad [7]$$

2.2.2.3 Copolymer synthesis

The cellulose acetate prepolymer was dissolved in 20 cc ethylene chloride and vigorously stirred. HPL and the catalyst (0.1% in total weight) were added. The total weight of HPL and CTA was kept constant at 2 g. The mixture was stirred and heated at 60°C for one hour. Films were cast directly from a 10% solution in ethylene chloride on Teflon plates. The plates were left under the hood for 12 hours so that the solvent was evaporating slowly. Then, the films were cured in an oven at 100°C for 12 hours. They were kept in a desiccator for one week before testing.

Analysis: DSC was performed on the copolymer samples in the following way. The samples were heated to 240°C - 260°C at 100°C/min and quenched to room temperature before scanning at 20°C/min.

Swelling studies were performed in DMF. The material (initial weight = I) was mixed with the solvent (10 cc) and left standing for 5 days before weighing the amount of swollen material (I_{gs}). The insoluble component was left dry for few days in a desiccator and weighed until a constant weight (I_{gd}) was obtained. The percentage of swollen material, SW or percentage of "weight gain upon swelling" was calculated as:

$$SW = (I_{gs} - I_{gd}) / I_{gd} \quad [8]$$

The percentage of soluble material or sol fraction was calculated as:

$$\text{Sol fraction} = (I - I_{gd}) / I \quad [9]$$

Morphological characteristics were studied on the films by wide angle X-ray scattering (WAXS). WAXS was performed on a PW 1720 X-ray generator. The operation conditions were a voltage of 40 kV and an intensity of 20 mA. Polymer films were mounted on the holders and submitted to the X-ray beams for 24 hours. The diffraction X-ray patterns were recorded on flat films.

3.0 RESULTS AND DISCUSSION

3.1 BLOCK COPOLYMER SYNTHESIS

3.1.1 CELLULOSE ACETATE COMPONENT

3.1.1.1 Parent CTA (*starting material*)

The commercial CTA had an acetyl content of 43.17% calculated from Eq.1. This indicates a degree of acetyl substitution, n , of 2.8 according to Eq.2.

The Infrared spectra of parent CTA and carbanilated CTA (phenylmonoisocyanate capped CTA), (Fig.7) indicate the disappearance of the hydroxyl absorption band at 3500 cm^{-1} and the appearance of the N-H stretching band at 1550 cm^{-1} as well as the C=C absorption band at 1600 cm^{-1} . This clearly shows that the CTA hydroxyl groups have reacted with the phenylisocyanate and that no more than trace quantities of OH groups remain unreacted. Figures 8A and 8B show the relationship between the carbanilate content, C , as a function of the absorbance, A , and the hydroxyl content (OH (%)). The ultraviolet spectrum of the phenylisocyanate-capped CTA shown in Fig.9 indicates an absorbance of 0.33 at 280 nm which leads to the value

of 0.855 % for the hydroxyl content of the parent CTA on a basis of a carbanilate content of 5.643 %.

The molecular weight of a monosaccharidic repeat unit, M_u , is 279.6 g/mole (from $M_u = 162 + 42n$, with $n=2.8$). From this, the number of hydroxyl groups per repeat unit, $nOH/unit$, is calculated as 0.14 (from Eq.5). The total degree of substitution is, therefore, $0.14 + 2.8 = 2.94$, and this is in fair agreement with the theoretical value of 3. The difference is probably within the limits of error of the analytical methods used.

Intrinsic viscosity measurements were performed in $CH_2Cl_2/MeOH$ (9/1 w) at 25°C. Under these conditions, the Mark-Houwink equation is given by (60):

$$[\mu] = 0.0156 [DP]^{0.834} \quad [10]$$

This equation can be transformed to give:

$$[DP] = 147 [\mu]^{1.2} \quad [11]$$

Figure 10 shows the linear relationship between $\frac{\mu_{sp}}{C}$ and C , where μ_{sp} is the specific viscosity and C , the concentration expressed in g/dl. The intercept at infinite dilute solution calculated by linear regression gives the intrinsic viscosity, $[\mu]$ as:

$$[\mu] = 2.086 \text{ dl/g}$$

This leads to a DP of 355 (from Eq.11) and to the average molecular weight $\bar{M}_n = 99258 \text{ g/mole}$ (from $\bar{M}_n = M_u \times DP$ and $M_u = 279.6 \text{ g/mole}$). From Eq.4, $nOH/mole$ of parent CTA is calculated as 50.

Figure 11 shows the DSC thermogram of the parent CTA. Four transitions are observed. These are : (a) an endothermic transition at $T_{max} = 90^\circ C$, (b) an exo-endothermic transition at $T = 183.8^\circ C$, (c) an exothermic transition at $T_{min} = 215^\circ C$, (d)

an endothermic transition at $T_{\max} = 296.15^{\circ}\text{C}$. Those transitions have been previously assigned (62) to : (a) softening and conformational rearrangement in the glucose ring and probably between two units themselves ; (b) T_g of the amorphous phase where large scales motions between chains begin to occur ; (c) the exothermic reaction of crystallization occurring upon heating the material, and (d) the melting temperature. The value of the heat of fusion calculated as $\Delta H_m = 5.6 \text{ cal/g}$, agrees with the value observed from the literature. Cowie (63) found values between 5.9 and 6.7 cal/g for fully substituted CTA of molecular weight between 62,000 and 100,000 g/mole. But, unfortunately, no values for the heat of fusion of completely crystalline CTA have been reported in the literature. Thus only relative crystallinities can be estimated.

The DMTA results of CTA are shown in Fig.12. A small transition is detected at approximately 90°C . This can be related to the first transition observed in DSC at the same temperature. At this temperature, the modulus drops slightly. At 194°C , the $\tan \delta$ peak is attributed to the T_g . The modulus drops considerably because the material changes from its glassy state to its rubbery state. After this transition, the modulus increases again and remains constant at a level intermediate between the modulus of the immediate pre- and post- T_g temperature. This can be explained by the fact that partial organization and crystallization occurs which results in a higher modulus. A rise in modulus at ca. 175°C suggests ample reorganization of chains during the glass transition at which mobility is favored.

All the information obtained from the analysis of the parent CTA is summarized in Appendix I.

3.1.1.2 CTA oligomers

Parent CTA depolymerization was first studied in a series of reactions in which the DP was measured as a function of time. The results are shown in Fig.13. The degree of polymerization, DP, drops very fast and then a plateau is reached. After 30 hours of reaction, the DP remains constant at 10. The influence of water added at the end of the depolymerization reaction on hydroxyl content produced a surprising result which is illustrated in Fig.14. The more the reaction time is increased the more it is difficult to obtain a high OH content. For 20 hours of depolymerization, an increase of the amount of water from 0.1 cc to 0.2 cc results in an increase of OH functionality from 2 to 3. The 32 and 46 hour reactions do not reveal a similar increase in OH content. A plateau is reached at ca.2 hydroxyl equivalents per mole of CTA. This can be explained with the fact that under the conditions chosen, macrocycle formation occurs resulting in a depletion of terminal OH groups. When increasing the time of depolymerization, more macrocycles are probably formed, and they prevent further cleavage of the CTA chain. Moreover, the existence of those stable macrocycles will not allow further reaction with water. Macrocycle formation has already been used by Steinmann (41) to explain the fact that a low hydroxyl content is obtained using this system of depolymerization. But, since then, no further investigations have been made to support this hypothesis. Despite that, this can therefore explain why a maximum OH functionality is reached after 32 and 46 hours (Fig.14). The DP plateau is not yet reached after 20 hours, which means that the macrocycles are not formed or not stabilized, and even a small variation of water added has a dramatic effect on the OH functionality. The conditions chosen for the depolymerization were expected to give a lower degree of OH content, and this was selected for this reason. It is, therefore, fortunate to discover that the results are in agreement with the intended purpose because this research emphasizes the synthesis of

a dihydroxy-end functionality CTA block. The alternative method described in the Objectives and Justification Section using H_2SO_4/H_2O system would have produced CTA blocks with higher OH functionality, higher degree of deacetylation, as it has been shown by Steinmann's work (41), and this conflicts with the goal of this study.

Finally, the method selected appears to be adequate, and four different CTA oligomers were selected for use in the prepolymer synthesis. These oligomeric fractions are identified as C46, C20, C32 and C5 in Table I, upper part. The letter 'C' stands for cellulose and the number refers to the time of depolymerization required to obtain these fractions from the parent CTA (ie: C20 is the oligomeric fraction obtained after 20 hours of depolymerization of the parent CTA (DP= 355) and having a DP of 20 as expressed in Table I). The different characteristics, \bar{M}_n , DP, nOH/mole, OH content (OH(%)) for each CTA oligomers calculated according to the methods described appear in this Table.

3.1.1.3 CTA prepolymers (TDI-capped CTA oligomers)

The lower part of Table I summarizes the characteristics of the different TDI-capped oligomers. Those prepolymers are identified as TC46, TC20, TC32 (ie: TC46 is the prepolymer obtained from the TDI capping of the fraction C46 previously defined). The oligomer C20 treated at 50°C for 4 hours gave the product TC20 with good results and no chain extension, the prepolymer and the oligomer having the same DP of 20. But some of the hydroxyl groups have remained unreacted. Indeed, starting with C20 (2.9 OH equivalent / mole) the prepolymer obtained, TC20 only has 2 NCO equivalent / mole. The same observation is made with the oligomer C32. When the reaction conditions are 25°C for 2.5 hours, no or very little chain extension occurred. The initial DP of 10 changes to 12 after the reaction. Similarly to what was observed

with the C20 compound, the prepolymer TC32 obtained from C32 (1.9 OH equivalent / mole) only has 0.9 NCO equivalent / mole.

The infrared spectra of the compounds C20 and TC20 (Fig.15) support this point. The absorption band at 3500 cm^{-1} due to OH vibration for C20 has not completely disappeared in the sample TC20. Those spectra also show the appearance of an absorption band at 2272 cm^{-1} which is due to the N=C=O vibration. The band at 1600 cm^{-1} is due to C=C (from TDI) vibration and the bands at 1550 cm^{-1} and 3330 cm^{-1} are due to -N-H vibration. The assignment of the other bands is shown in Table II. The observation of hydroxyl bands in the two spectra (Fig.15) confirms the suspicion that not all the hydroxyl groups can be carbanilated. This could be due to the difference in reactivity and the steric hindrance of the CTA hydroxyl groups or to an incomplete reaction for some other reason. When operating at higher temperature and time with oligomer C46, chain extension occurs, the DP going from 10 to 20. However, the OH equivalent/mole of C46 remains the same as the NCO equivalent / mole of TC46 at a value very close to 2. Therefore, it appears that a compromise must exist within the TDI capping reaction regarding the time and temperature conditions with respect to a complete substitution of the OH groups. This point is obviously observed when one look at the influence of the conditions applied (ie: time and temperature) on the two oligomeric fractions C46 and C32 having the same initial DP of 10. If the time and temperature conditions of the TDI capping reaction are high (ie: 50°C and 4 hours applied on C46), the same OH and NCO equivalent are obtained but chain extension occurs. On the other hand, if those conditions are lower (ie: 25°C and 2.5 hours applied on C32) chain extension is very much minimized but some hydroxyl groups remain unreacted. This is the reason why optimum conditions had to be defined to master the contribution between the preservation of a DP and a sufficiently high NCO functionality (ie: 2 NCO equivalent / mole).

Different capping conditions were tested for each oligomer and the best are listed in Table I. Trial reactions made on C20 at 25°C for 2 to 3 hours gave prepolymers with an NCO functionality of less than 0.5 which was too low. With respect to TC46, even though chain extension occurred, the NCO functionality (2 NCO equivalent / mole) is acceptable in terms of what the goal of this research is. This is the reason why the prepolymers TC46 and TC20 were selected for the synthesis of the block copolymers. With respect to prepolymer TC32, in spite of its lower NCO content it was also selected because the DP was preserved at a value of 10 compared to TC46 and TC20 having a DP of 20. Therefore, two different sizes of cellulose block were available. Attempts to improve the NCO content of TC32 were made but did not produce better results. Finally, it was impossible to obtain prepolymers with a DP of 45 although oligomers C5 (DP=45) were generated by the depolymerization of the parent CTA after 5 hours of reaction. Various TDI capping conditions applied to this compound produced products which were insoluble in the common solvents. This can be attributed to their high OH content (ie: 9 OH equivalent / mole). This OH abundance likely induced crosslinking during the TDI capping reaction. Therefore, this sample was not further investigated. In addition to that, this observation leads to another explanation for the incomplete substitution of the hydroxyls. It is likely that some hydroxyls are involved in crosslinking reactions within the cellulosic chains through the two NCO groups of TDI which explains why lower values are observed for the NCO equivalent / mole compared to the values of the OH equivalent / mole of the initial material.

Finally, TC46, TC32 and TC20 were the three isocyanate capped polysaccharide blocks selected for reaction with HPL. DSC thermograms of TC20 and TC32 are shown in Fig.16. Those curves are observed after a second scan. An endothermic peak characteristic of the heat of fusion was observed on the first scan for the two compounds. Therefore, the following standard procedure for DSC experiments was chosen in order

to compare all results on initial amorphous compounds. The melting temperatures observed for TC20 and TC32 after the first scan at 20°C/min were 260°C and 240°C, respectively. Therefore, the samples were first heated at 100°C/min up to the melting point and quenched. The DSC thermogram of TC46 is not shown here because it was exactly the same as that of TC20. Figure 16 indicates that even depolymerized cellulose acetate remains crystalline since a peak of fusion is observed. Moreover, they clearly show the endothermic transition at T_g . The endothermic peak at 70°C observed for TC20 can be attributed to conformational reorganization of the glucose ring as it was observed for the parent CTA. This feature does not occur anymore for TC32 because of the short segment size. The values obtained from the DSC experiments performed on the prepolymers are summarized in Table III. This table also lists the values obtained for the parent CTA whose DSC thermogram is shown in Fig.11. The values for the melting point of the prepolymers compounds (274.25°C and 263.51°C) are lower than that of the parent CTA (296.15°C). This is due to a diluent effect and to the decrease in molecular weight ; the prepolymers are no longer pure, high molecular weight cellulose but rather a product of degradation and diisocyanate reaction. The effect of TDI (probably acting as a plasticizer) and the reduction in molecular weight also reduces the T_g values (136.63°C and 173.31°C) compared to 183.8°C for the parent CTA. The lower values of T_g and T_m observed for the TC32 compound as compared to the TC46 and TC20 compounds are due to the decrease in DP. However, it is surprising to observe that the heat of fusion, ΔH_m , of TC32 is higher than that of TC20 and TC46 even though the DP of the former is lower. This fact will be discussed in the following section.

3.1.2 HYDROXY PROPYL LIGNIN COMPONENT

Hydroxypropyl lignin had been prepared previously. Therefore, only few words will be said about its synthesis. The interested reader is referred to different publications on this subject (23, 54, 55, 56). In brief, the hydroxypropylation of lignin had been carried out in a batch reactor under alkaline conditions at 180°C for about 90 minutes. The reactor content had been collected by dissolution in methanol or acetonitrile and extracted with hexane. Hydroxypropyl lignin had been obtained by precipitation of the acetonitrile solution in water. Its characteristics regarding chemical and molecular structure were determined as 6.06 % for the hydroxyl content (from the method already described) and the molecular weight (\bar{M}_n) determined by VPO as 2615 g/mole.

Figure 17 shows the plot $\Delta T / C$ versus C obtained from the VPO experiment. \bar{M}_n , is calculated by $\bar{M}_n = K/I_s$; where, I_s , is the intercept of the curve at infinite dilution. This is determined as 2.052 by linear regression, and K is a coefficient given by the calibration curve obtained from benzil, the reference compound. The details of the procedure employed to calculate K are illustrated in Appendix II.

The DSC thermogram shown in Fig.18-a) indicates a T_g of 80.3°C. The shape of this curve agrees with the amorphous nature of HPL. A summary of its characteristics is shown also in Appendix I.

3.1.3 BLOCK COPOLYMERIZATION

Formulation parameters for the block copolymerization are shown in Table IV. The samples are designated under three series. The series P46 relates to the copolymers

obtained from prepolymer TC46. The last two numbers appearing in the identification relate to the molar OH/NCO ratio. For example, the sample designated by P4612 is the copolymer made from TC46 with a molar OH/NCO ratio of 12. The same designation is adopted for the series P20 (ie: P2008 stands for the copolymer made from TC20 with a OH/NCO ratio of 8). However, for the series P32 the first two numbers relates to the initial prepolymer (ie: TC32), but the last two numbers relate to the HPL content. Therefore, P3220 is the copolymer obtained from TC32 containing 20% of HPL in weight.

The films were obtained by direct casting from solution which is usually the procedure employed to minimize gel formation. Attempts to solubilize the prepolymers showed that dichloroethane-1,2 was best qualified. In addition, HPL was also soluble in this solvent, and the low boiling point was considered an advantage. This accounts for the choice of this solvent. Dibutyltin-dilaurate is a common catalyst used in polyurethane synthesis, and this has already been selected in many synthesis of lignin based polyurethanes. It proved to activate the reaction well. The selection for HPL content was dictated by stoichiometric requirements, because of its high OH functionality, and these ranged from 5% to 55%. It is expected that crosslinking reaction will be minimized. It is, therefore, evident that since the number of NCO equivalent of the CTA prepolymers is low compared to the number of OH equivalent of HPL block, the molar OH/NCO ratios of all samples are greater than 1.

3.2 BLOCK COPOLYMER PROPERTIES

The copolymer films obtained were clear, glassy and very brittle. The glassy nature made it impossible to conduct thermal analysis (modulus or $\tan \delta$) or stress-strain testing. However, thermal properties and network morphology were tested by DSC and swelling. In addition, wide angle X-ray scattering was performed on the films.

Three DSC thermograms (obtained after an initial scan through T_m), each for a sample in the series P46, P20 and P32, are shown in Fig.18. A glass transition at T_g , a small broad crystallization peak at T_c (temperature of crystallization) and, an endothermic peak of fusion at T_m , are displayed with more or less intensity by all three thermograms. Within the same series, the curves have exactly the same shape except that the values are shifted. All the parameters obtained from the DSC experiments, the values of T_g designated by " T_g experimental ", T_m , and the heats of fusion, ΔH_m (area under the endothermic peak of fusion) for each copolymers are shown in Table V. In Fig.19, the relationship between HPL content and " T_g experimental" is plotted according to the values given in Table V. In Figure 20, the relationship between the heat of fusion and the cellulose content is also given according to the values of Table V. The results obtained from the swelling studies are shown in Table VI according to Eq.8 and 9. The sol fraction (%) is plotted as a function of the cellulose content in Fig.21.

The DSC thermograms (Fig.18) clearly show single T_g values. These values are between 100°C and 140°C and consequently are between the T_g values of the two homopolymers TC and HPL. Figure 19 indicates that T_g values and HPL content are related and T_g decreases as HPL content increases. The T_g values of the P32 series, composed of a cellulose block of DP= 12, are lower than that of the P46 and P20 series, composed of a cellulose block of DP= 20 (Fig.19, Table V). This is due to the difference

in size of the cellulose blocks. If this size decreases, the T_g value decreases. It is interesting to compare those experimental results with the model of Fox (64) which predicts the T_g of a random copolymer according to the following equation:

$$\frac{1}{T_g} = \frac{W_1}{T_{g1}} + \frac{W_2}{T_{g2}} \quad [12]$$

where T_g is the glass transition temperature of the copolymer, T_{g1} and T_{g2} are the glass transition temperatures of each homopolymer, and W_1 and W_2 , are the weight fraction of each homopolymer in the copolymer composition. For the P20 and P46 series and the P32 series, the T_g values of the pure polysaccharide blocks were obtained by DSC as 173.31°C and 136.63°C respectively (Table III). Knowing these values, the T_g value of the HPL block (80.3°C) and the HPL content of each copolymer, the theoretical T_g values of the copolymers were calculated according to Eq.12. Those values are expressed in Table V as " T_g theoretical". Furthermore, these values were plotted as a function of HPL content in Fig.19. A consistent variation between the experimental results and the theoretical model is revealed, which accounts for non randomness of the copolymer structures. This agrees with the goal of synthesizing a block rather than a random copolymer and with the existence of crystallinity detected by DSC and accounted for by the existence of an endothermic peak of fusion which is proportional to the degree of crystallinity of the copolymer.

It is recognized that the copolymers are composed of three components: amorphous lignin, amorphous cellulose and crystalline cellulose. In this system, the two closely associated amorphous components exhibit one single T_g value while, the crystalline cellulose induces phase separation and is the basis of crystalline domains accounting for a block structure. Reports from the literature (65), based on the study of the crystallization of block copoly (ether ester) have also revealed a single T_g value

leading to the same conclusion. However, one must not omit that the DSC detection of one single T_g can be due to the short size of the two blocks (ie: TC and HPL) and that if those sizes were longer, two separate T_g could be detected. There is not a great variation in the T_m values of the copolymers in each series as shown in Table V. These values are between 283°C and 254°C for the copolymers of the P20 and P46 series and lower, between 246°C and 252°C for those of the P32 series. However, these melting temperatures, influenced by the cellulose block length, are lower than the T_m values of the cellulose prepolymer blocks (Table III), and obviously lower than that of the parent CTA. This result also agrees with the dilution effect attributed to the introduction of the lignin component and the diisocyanate in the cellulose component. In a recent paper, Droscher (65), who studied the crystallization behavior of block copoly (ether ester), showed that the melting temperatures of the compounds were not anymore influenced by the crystallizable segment length when this length was increased (above 12 units). This supports the argument that big variations in the T_m values fail to be observed because the length of the cellulose segments exceeds the maximum length beyond which T_m values do not vary.

Since the crystallization behavior of the copolymers is attributed to the crystallizable cellulose CTA block, it was interesting to consider whether the heat of fusion and the cellulose content were related. This relationship is shown in Fig.20. This figure clearly shows that the heats of fusion are higher for the copolymers having longer length segments. The extrapolation of the two curves at 100% cellulose gave respectively values of ΔH_m as 2.3 cal/g for P46 and P20, and 3.6 cal/g for P32. These values agree with the values obtained from the DSC experiments performed on the prepolymers TC46, TC20 and TC32 (Table III). Except for the 100 % composition, the copolymers of the P20 and P46 series composed of cellulose block of DP 20 are more crystalline than the copolymers of the P32 series which are composed of cellulose block of DP 10. This

can be explained with the fact that the shorter cellulose chains, in the samples of the P32 series, mix better with HPL since the two components have the same order of molecular weight and have less tendency to restrict each others mobility. Therefore, the occurrence of domains is minimized which induces less crystallinity. On the other hand, with the two other series, the tendency of the cellulose to mix with HPL is minimized because of the greater chain length. It can be thought that their mobility is restricted so that the cellulose chains remain more associated with each other. Therefore, domains occur more easily and the crystalline phase is better developed. In addition, it is observed (Fig.20) that the higher the cellulose content the higher the heat of fusion and consequently the higher the degree of crystallinity. This observation suggests that network structure is not developed in the samples and that crosslinking reaction has probably be minimized. To verify that, it was of interest to estimate the degree of crosslinking of the system. This was done by studying the swelling properties of the block copolymers.

The results from the swelling experiments calculated according to Eq.8 and 9 are represented in Table VI, and the percentage of soluble material (sol fraction) was plotted versus the cellulose content in Fig.21. The sol fractions are surprisingly high between 40% and 90%. But, these values and the high degree of swelling confirm the low degree of crosslinking present in all the samples. In fact, the copolymers of the P32 series do not seem to be networks at all, and this agrees with the fact that their cellulose blocks had a NCO equivalent per block length of 1. However, the percentage of soluble material and of swollen material slightly decreases with an increase of the cellulose content. This cannot be explained in terms of degree of crosslinking but rather by the crystalline character of the samples which seems to be the dominant factor. Indeed, when the cellulose content increases, the degree of crystallinity of the samples increases from the observation of Fig.20 and, therefore, it is possible that the samples become more difficult to dissolve as observed in Fig.21.

These results regarding crystallinity are quite surprising because the copolymers consist of quite short crystallizable segments that form a crosslinked network. However, crystallinity of cellulose blocks even for short DP in block copolymers has already been mentioned in several papers (44,46). Mezger (44) stated that the high tendency of the cellulose triester to crystallize facilitates phase separation. Feger (46) observed phase separation in star block copolymers. This suggests that crystallinity in copolymers from cellulose acetate is common. Those authors also observed a contribution of network formation on crystallization behavior. When the degree of crosslinking was low crystallinity behavior and phase separation were occurring. Therefore, it must be suspected that the synthetic methods employed favor the observations made on the lignin-carbohydrate blocks : Phase separation occurs in amorphous-crystalline block copolymers having the potential to crosslink but where the degree of crosslinking remains low. Crosslinking is minimized in the system due to the low NCO content of the prepolymers which can be assumed to be located at the end of the cellulose chains allowing crystallization to dominate, and due to the low HPL content. Crosslink density is expected to rise with HPL content because of its high functionality; but the conditions chosen resulted in the minimization of this factor.

Small angle X-ray scattering (SAXS) was performed on the copolymers but did not produce conclusive results. However, wide angle X-ray scattering (WAXS) was performed on the four samples P3220 (80% cell), P3240 (60% cell), P4604 (75% cell) and P4608 (60% cell). The results reveal interesting features (Fig.22). Very sharp, concentric, continuous and uniform rings are observed, characteristic of a crystalline phase and an external halo due to the scattering of the amorphous component. Moreover, the intensities of the rings are practically the same for the three samples P3220, P3240 and P4608. By contrast, the rings observed for the sample P4604 are much more intense. This is not surprising since P4604 is the copolymer having the highest heat of

fusion (ie: 1.68 cal/g) compared to the other copolymers (Fig.20 and Table V). Therefore, P4604 is the copolymer having the highest degree of crystallinity and, in an X-ray pattern, the more the sample is crystalline, the more the rings or spots are intense. Works conducted by Clark (66-68), in the study of the crystalline structure of cellulose, showed that an X-ray pattern made of continuous, concentric and uniform rings is produced by an aggregate of small grains or micelles in random orientation. Moreover, the sharpness of the rings are related to the size of the micelles. Clark (68) found that sharpness and uniformity are obtained when the diameter of the diffracting particles lies between 10^{-3} and 10^{-6} cm. If they are larger than 10^{-3} cm, the diffraction pattern becomes dashed and spotted as would be expected for larger single crystals. If the particles are smaller than 10^{-6} cm, the rings become broader in proportion to restriction of particle size. These observations are also valid for CTA in which high crystallinity has been recognized (44, 69). Therefore, the WAXS results allow to conclude that the copolymers are composed of an organized, totally randomly oriented crystalline structure¹. Their size can be estimated to be around 10^{-6} cm (100 Å). For the cellulose itself (70), the dimension of the crystallites have been estimated to be around 600 Å with a width between 50 and 150 Å. This corresponds to 4 anhydro-D-glucose repeat units per unit cell. The dimensions of the unit cell have been estimated at 10.3 Å, 8.35 Å and 7.9 Å (Fig.3) and usually, the X-ray pattern for CTA shows broader rings. This value of 100 Å seems high for short cellulose segments and may be explained by the better tendency of short chains to pack compared to high molecular weight chains. This would confirm why SAXS analysis fail to produce conclusive results ; SAXS is capable of detecting only short size domains of less than 140 Å overall dimension.

¹ X-ray diffraction of the prepolymer TC20, TC32 and TC46 display the same characteristic patterns (ie: sharp concentric rings). This supports that the crystallization obtained in the copolymers is due to the cellulosic blocks.

In addition, the samples were examined through a microscope equipped with a polarizing lens and a hot-stage. Transparent zones (crystalline) zones disappeared upon heating to the melting point but failed to appear again when annealed between 150°C and 200°C for one hour. This observation has already been made by Baker (69). Cellulose triacetate samples annealed at 150°C for 95 hours do not produce detectable crystallization. This emphasizes the high intermolecular forces existing in CTA which, at this temperature, restrict chain rotation. It can thus be concluded that HPL and CTA are linked together not only through valence bonds but also that they are closely associated through intermolecular forces. This explains why those two blocks are closely associated in their amorphous phases even though they have a very different chemistry.

This suggests that crystallization was initially present in the samples and that it occurred in the copolymers during the casting procedure from solution and prior to curing. In solution, the CTA chains diffuse through the lignin matrix and crystallize. Ability of CTA to crystallize from solution has often been observed (63, 69) and an influence of the solvent (69) on film properties has been reported. It has been observed that good solvents for CTA (ie: ethylene chlorohydrin) produced more brittle films, of higher crystallinity, than do poor solvents (ie: chloroform). Therefore, it is possible that ethylene chloride, a good solvent for CTA, enhances brittleness and crystallinity of the solvent cast copolymer films. The brittle character of the samples can also be explained by the brittle nature of the lignin component at room temperature and by the fact that the films are in their glassy state far below the T_g values. When the samples are heated, the brittleness disappears and the films can be easily cut without fracture. Upon cooling they become brittle again. Therefore, the following factors may be cited as reasons for the brittle nature of the samples:

- Nature of the solvent used in the casting procedure.

- Brittle nature of the HPL component.
- Crystalline nature of the CTA component.
- Nature of the copolymer made of two relatively hard segments.

By contrast, network structure is not expected to contribute to brittleness.

The fact that the 100% TC46 and TC20 cellulose blocks of (DP 20) are less crystalline than the 100% TC32 blocks of (DP= 12) (Fig.20) can, now, be readily justified. This can be explained by the lower degree of acetyl substitution (higher hydroxyl substitution) in the block of DP of 20 with respect to the block of DP of 12. This lower hydroxyl substitution in TC32 results in the minimization of the intermolecular forces which accounts for more mobility between the chains. From Cowie (63), cellulose triacetate (163,000 g/mole and $n = 2.8$) has a heat of fusion of 3.83 cal/g, while the value for CTA (62,500 g/mole and $n = 3$) is 6.70 cal/g. This shows that the degree of acetyl substitution plays an important role for the crystalline behavior. A lower degree of acetyl substitution induces a higher irregularity in the groups substituted on the backbone, which limits therefore their ability to organize. By contrast, if the degree of substitution is higher and more uniform, the substitutes can take a predictable orientation with respect to the others leading to a more organized structure and, therefore, to a higher degree of crystallinity. However, in solution with HPL the crystallization occurs more easily with high molecular weight chains during the casting procedure.

Similar polymer systems have been studied by Slowiskowska and Daniewska (71). These authors have determined the dependence of the crystallization capability of crosslinked polyethylene glycols and polyethylene sebacate polyurethanes. Shorter glycol chains between the junction points crystallized less easily when the degree of crosslinking was low because of the reduction of their degree of freedom. This accounts for the results found for HPL-CTA copolymers where shorter CTA blocks were less

crystalline than the corresponding longer CTA blocks. In addition, Gervais (72), in a study of block copolymers made of an amorphous component (polybutadiene) and a crystallizable component (polyethylene oxide, PEO), showed that the nature of the amorphous block was influencing the ability of the PEO chains to crystallize. According to this result, it can be postulated that HPL in HPL-CTA block copolymers acts as an amorphous surface available for the CTA chains to crystallize on, in solution.

4.0 CONCLUSIONS

Copolymers from NCO capped cellulose triacetate oligomers and HPL could be synthesized with a range of compositional parameters. Synthesis parameters were limited by difficulties encountered in the depolymerization of CTA to target sizes of cellulose blocks. However, this constitutes the first example of the synthesis of a multi-phase copolymer where all the components consisted of macromers from a natural polymer source. Therefore the following facts can be stated:

- It is possible to synthesize lignin-cellulose derivative block copolymers.
- Cellulose block length can be varied despite the difficulty existing with difunctionality.
- The properties of the copolymers are dictated by the glassiness of the components ; and by the crystallization of cellulose at all DP levels (down to 10). T_g values are very near the values predicted by Fox and the deviation comes from block nature induced by crystallizable segments.
- The properties are not influenced by network architecture since sol fractions are always above 40% and the factor influencing the properties is the crystalline character of the copolymers at any composition and molar OH/NCO ratio.
- Phase separation is achieved between an amorphous component composed of lignin and cellulose closely associated through valence bonds and intermolecular forces, and a crystalline phase made of organized micelles randomly oriented.

- The size of the crystalline domains is around 100 Å.

However, the brittle nature of the copolymers make this study incomplete in terms of their mechanical characteristics. Therefore, future studies can be proposed to optimize the synthesis of the block components and the block copolymers. These are:

- Systematic research where time and temperature are varied in the TDI capping reaction in order to understand how reaction conditions influence the final properties.
- Synthesize block copolymers with a "soft" lignin derivative block which already exists (49) and whose low T_g value would produce copolymers with lower T_g values : this can be expected to produce thermoplastic compounds.
- Develop a new approach in the chemistry to link lignin and cellulose.

In terms of the crystallization study by WAXS, one may recommend as a future work, to run X-ray diffraction patterns of the intermediate oligomeric cellulose fractions (C20 and C32 samples). Those results would help to definitely establish that the cellulosic blocks are the origin of the crystallization observed in the copolymers. Again, it must be emphasized that all compounds synthesized in this research are derived from a natural resource, and this is of great interest in term of a potential industrial application which needs to take environmental issues into consideration.

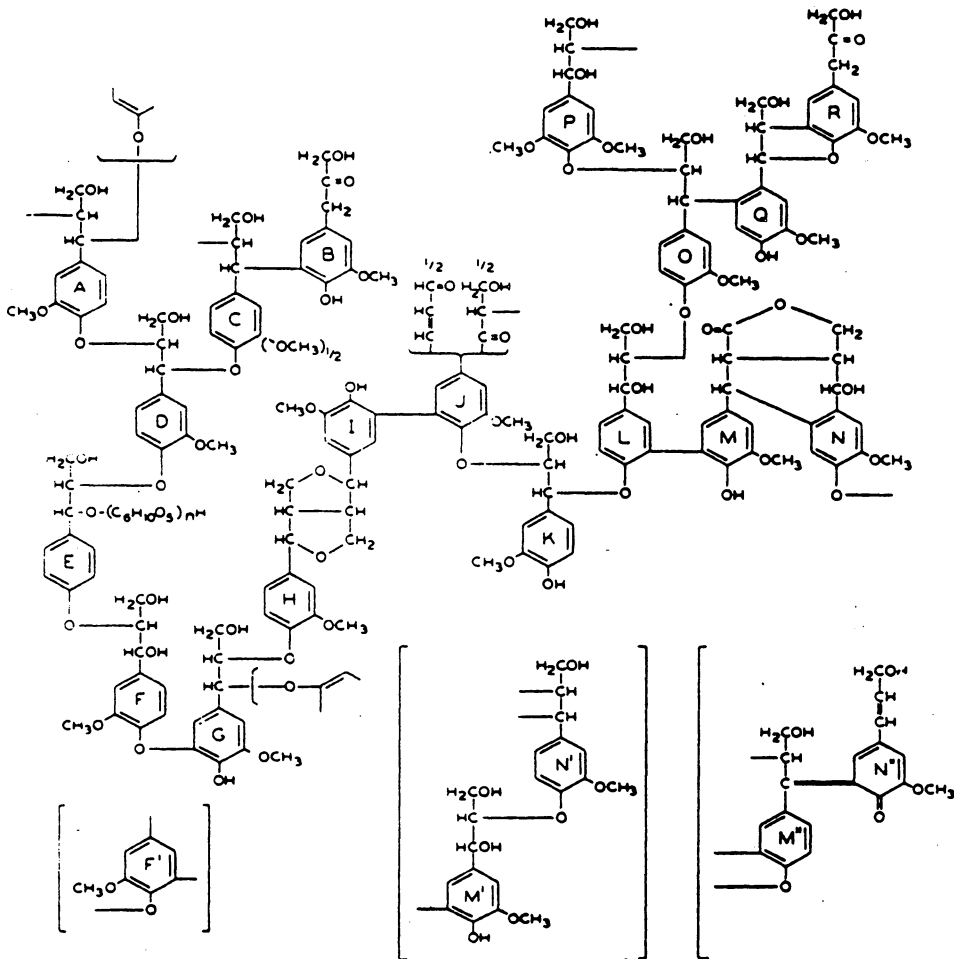


Figure 1: Schematic representation of a softwood lignin structure by Freudenberg (4).

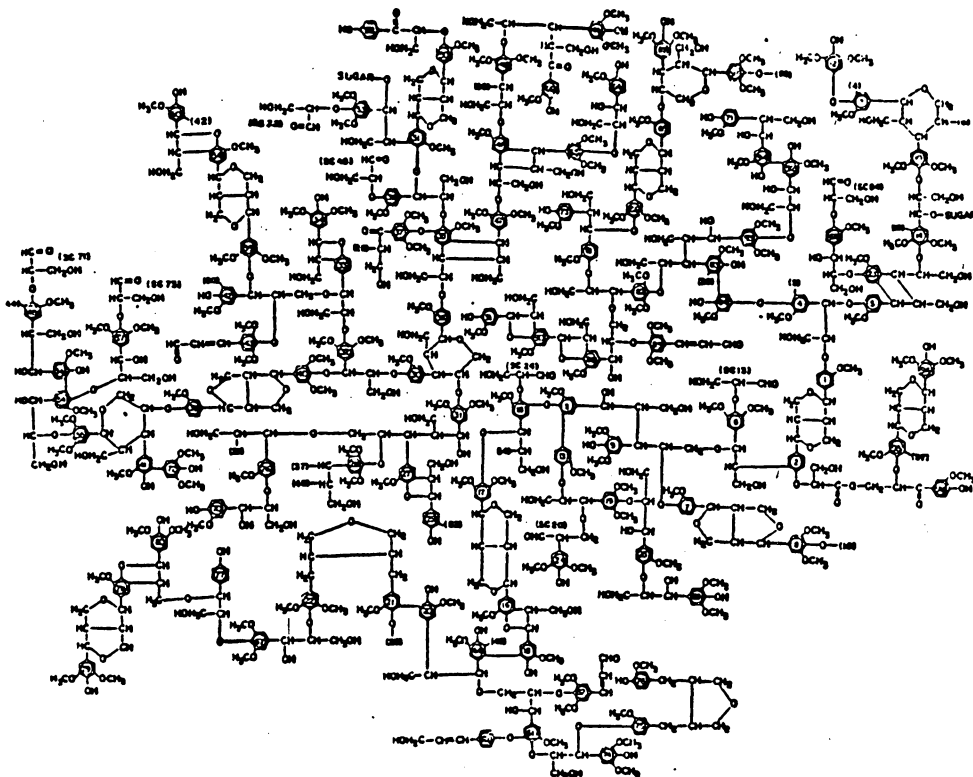


Figure 2: Schematic computer simulation structure for hardwood lignin by Glasser (8).

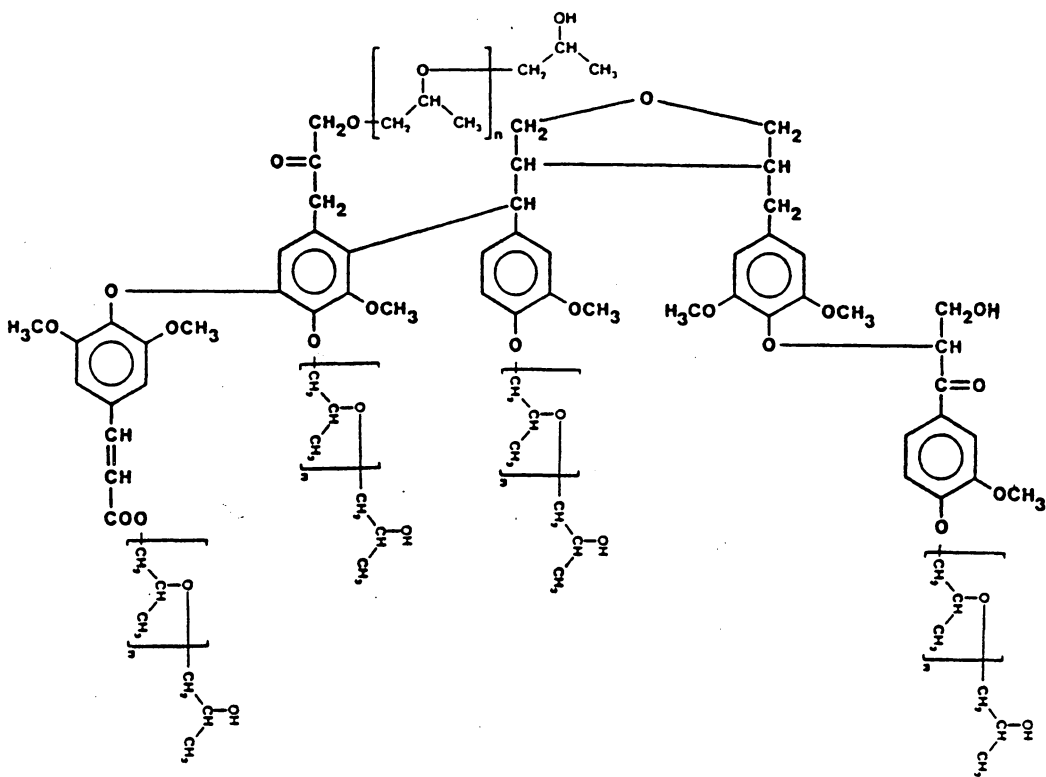


Figure 3: Schematic representation of a hydroxypropyl (organosolv) lignin derivative structure.

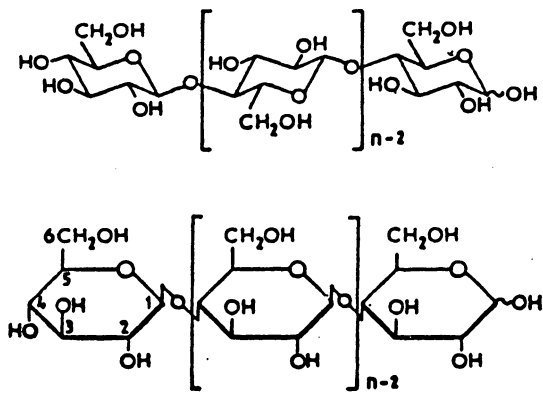


Figure 4A: Cellulose structure.

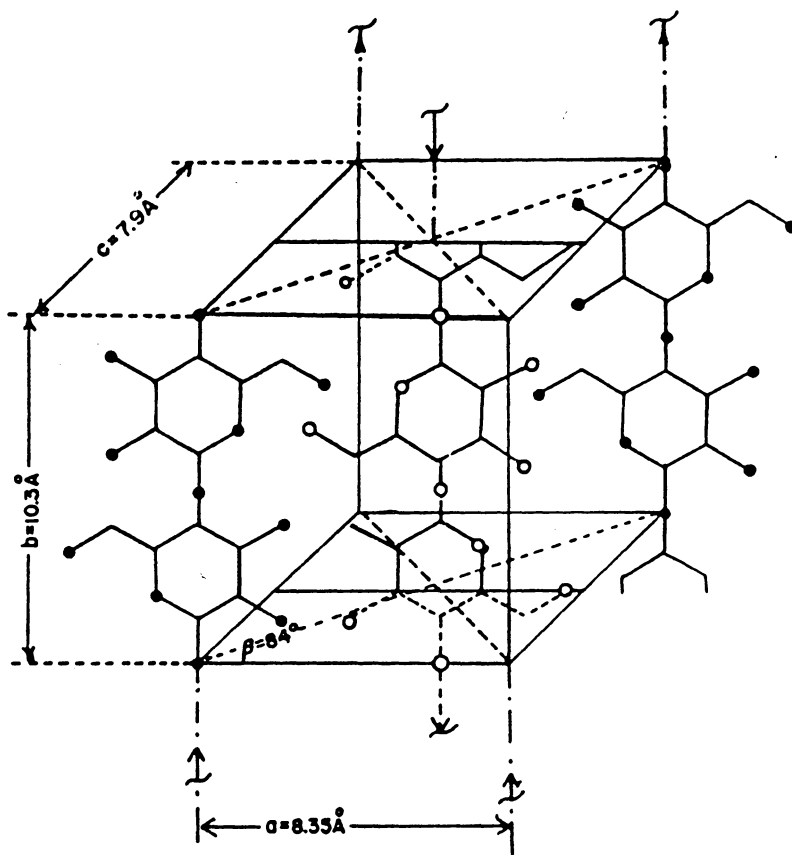


Figure 4B: The unit cell of native cellulose.

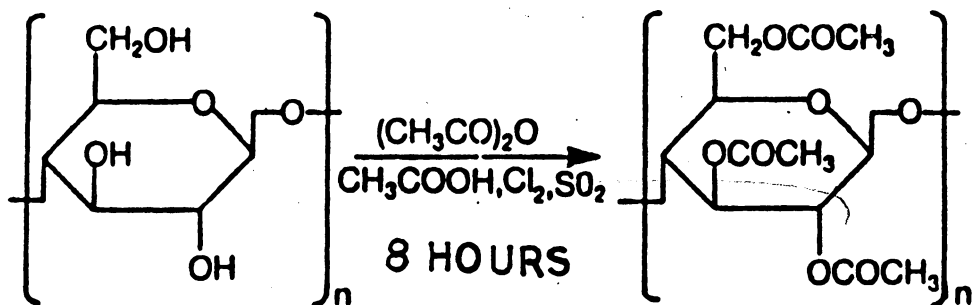


Figure 5A: Synthesis route for cellulose triacetate.

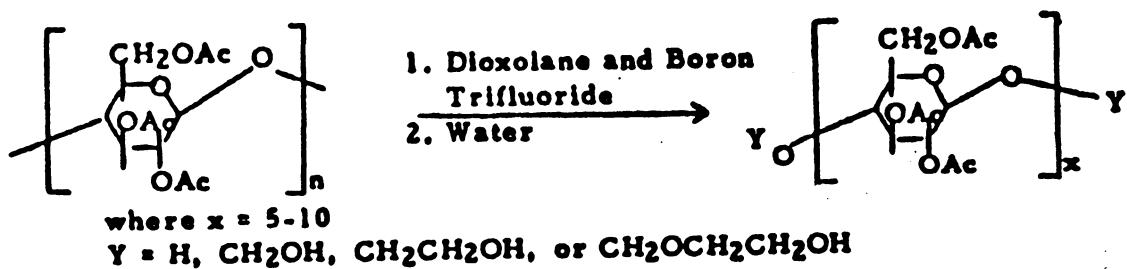


Figure 5B: Synthesis route for the depolymerization of cellulose triacetate.

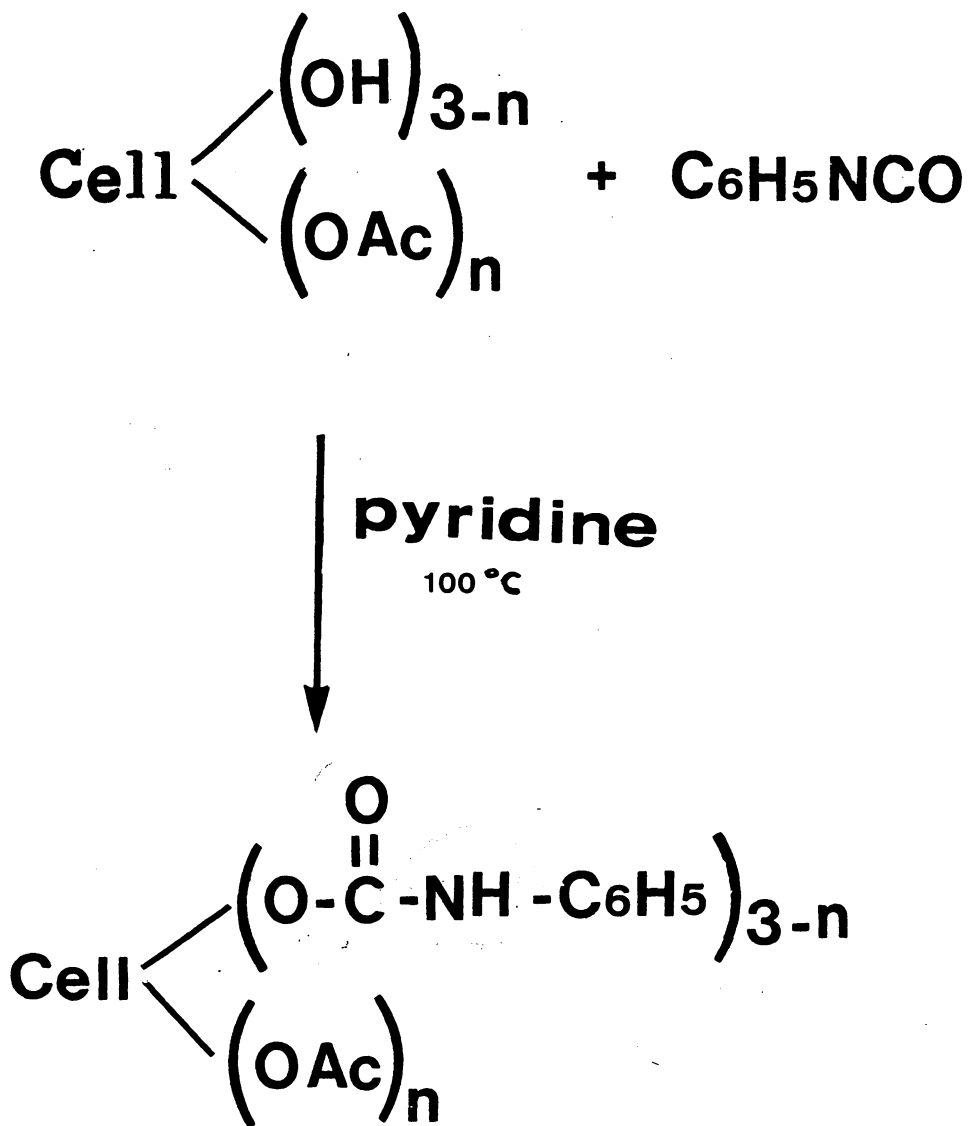


Figure 6: Synthesis route for phenyl-monoisocyanate capped cellulose triacetate.

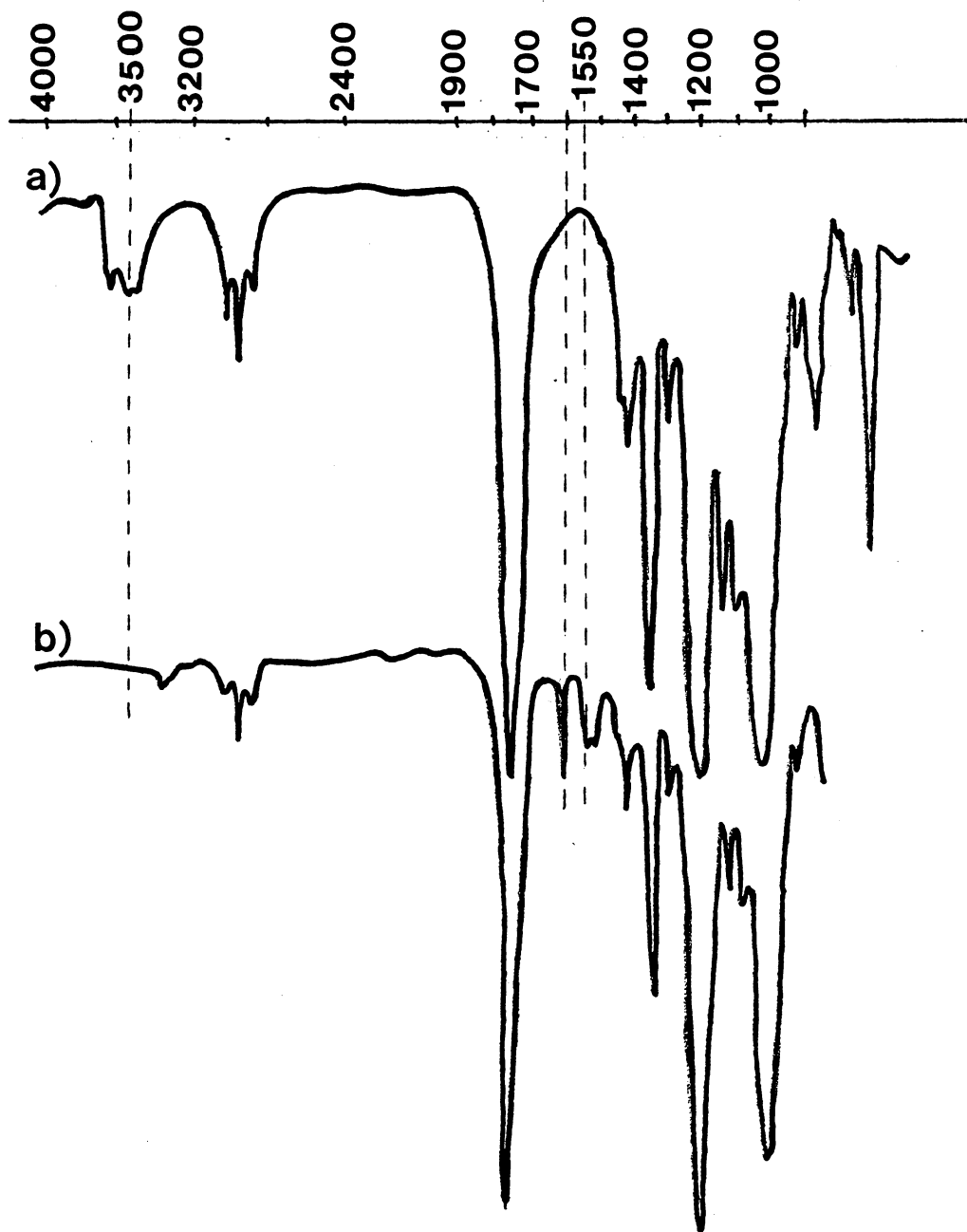


Figure 7:
Infrared spectrum of a) cellulose triacetate (CTA).
b) phenyl-monoisocyanate capped cellulose triacetate.

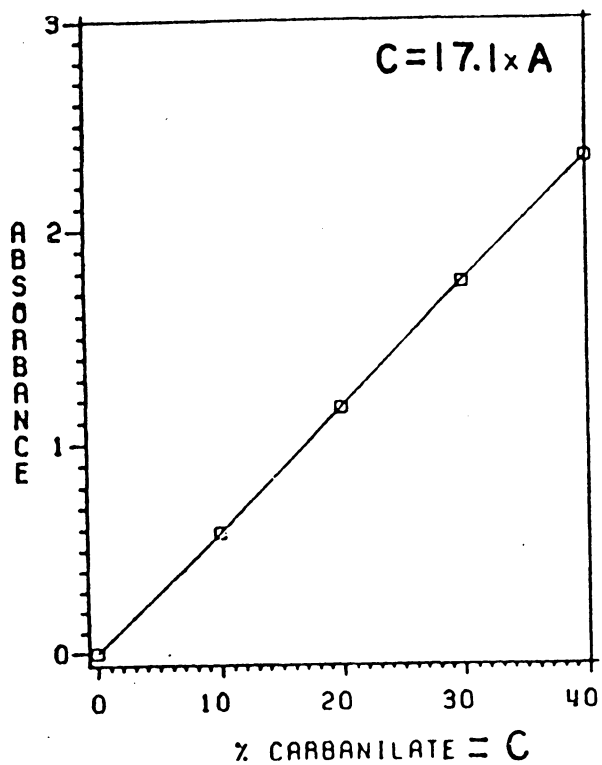


Figure 8A:

Relationship between carbanilate content and UV absorbance of phenyl-isocyanate capped cellulose triacetate.

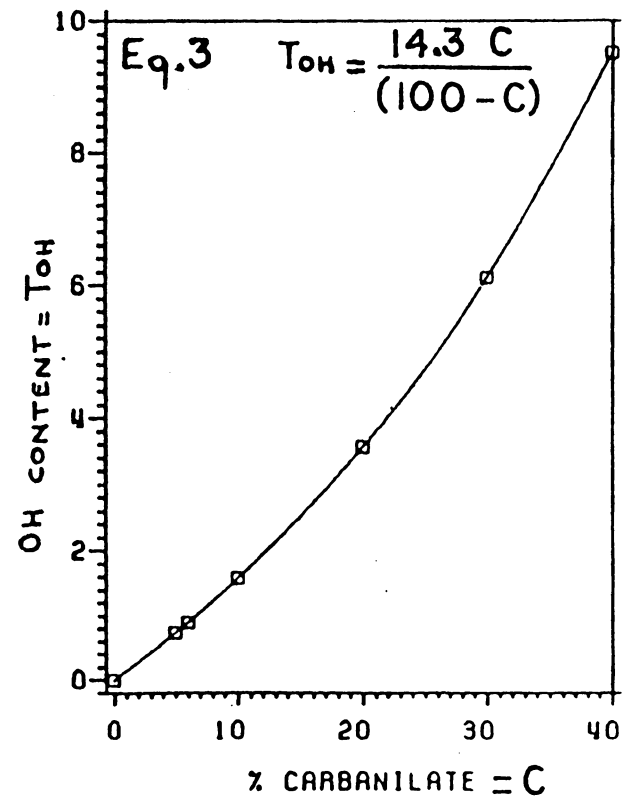


Figure 8B:

Relationship between carbanilate content and hydroxyl content.

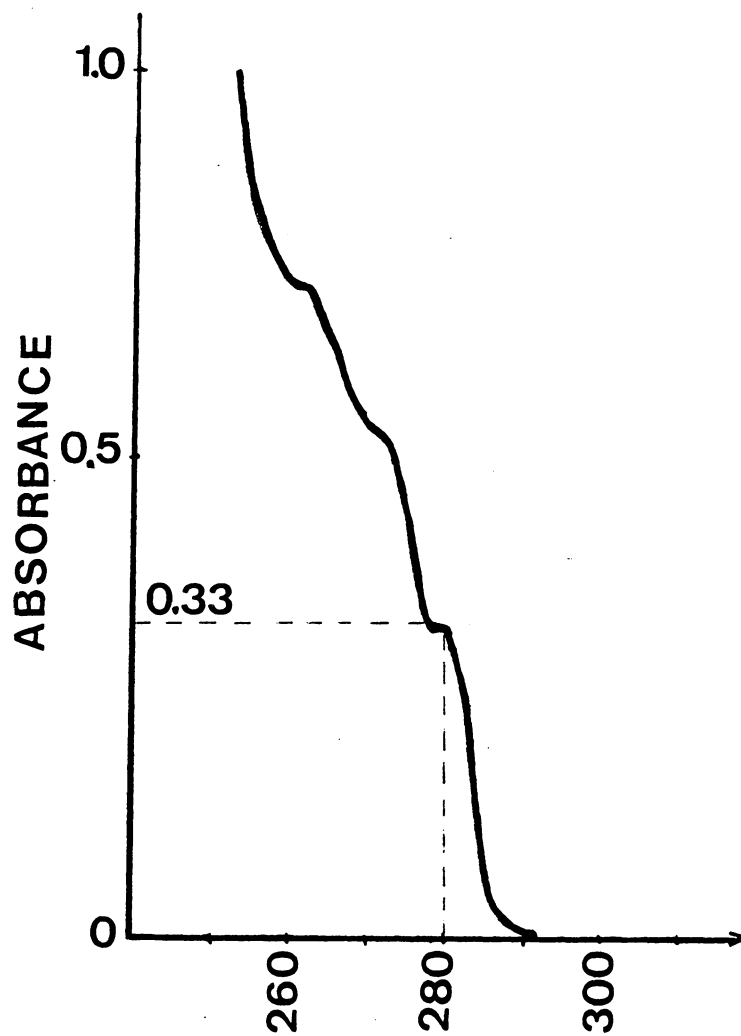


Figure 9: Ultraviolet spectrum of phenyl-monoisocyanate capped cellulose triacetate.

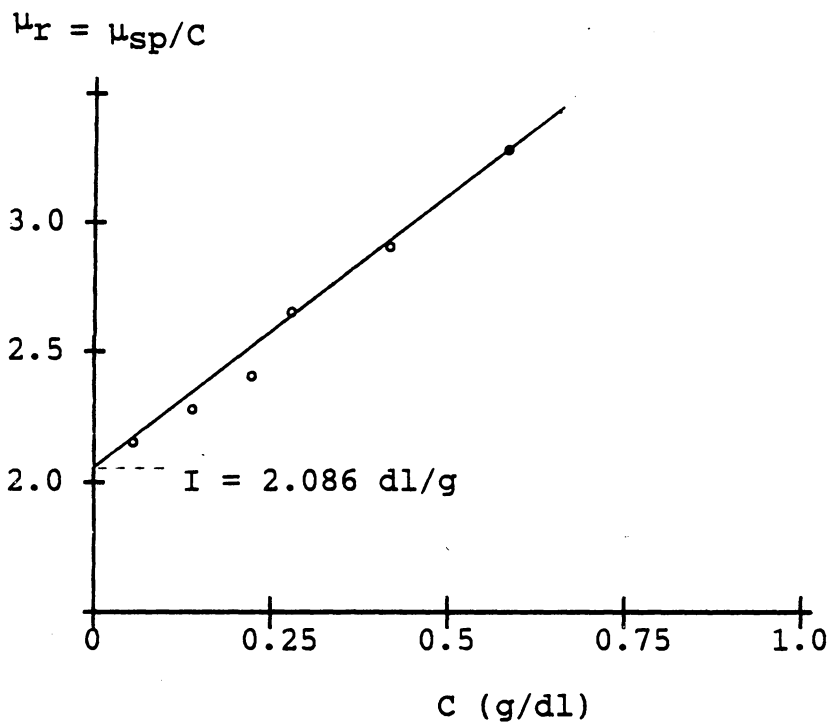


Figure 10: Relative viscosity versus concentration for Parent CTA.

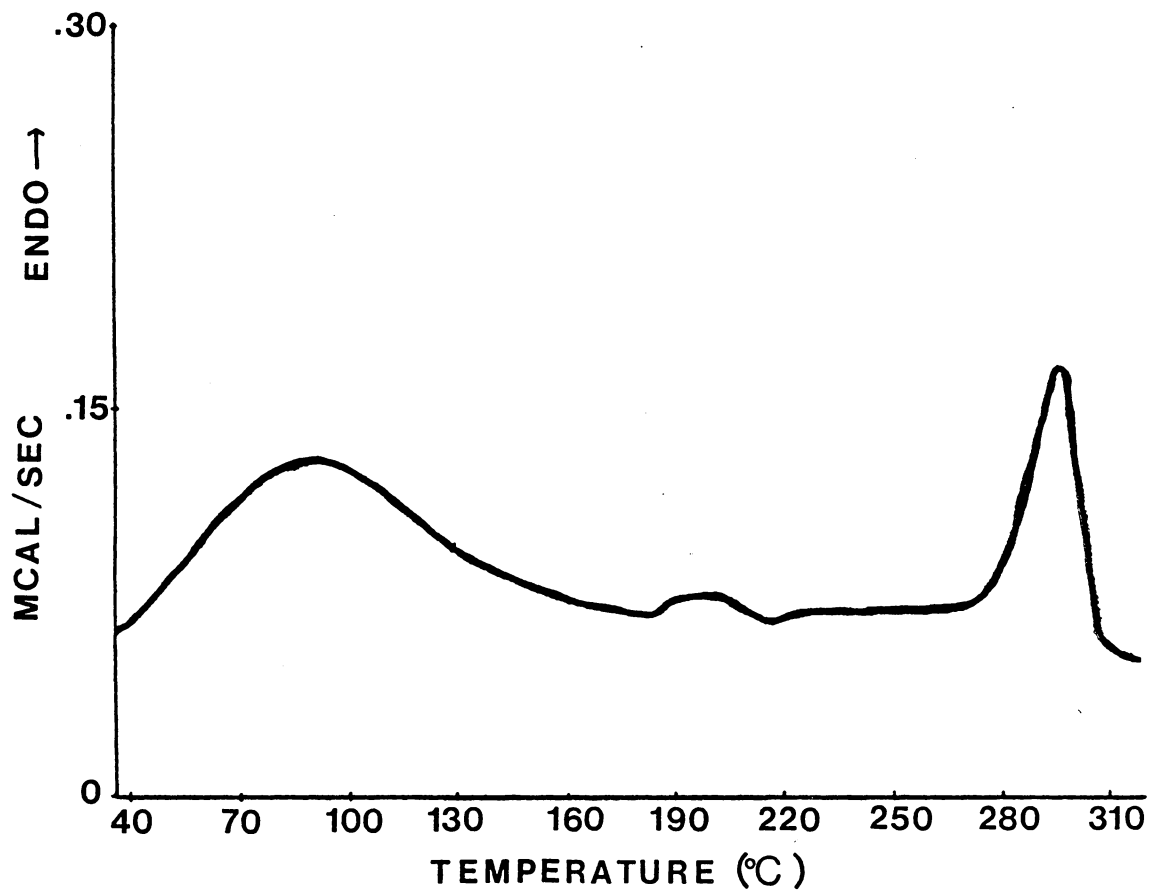


Figure 11: DSC thermogram of Parent CTA (DP = 355).

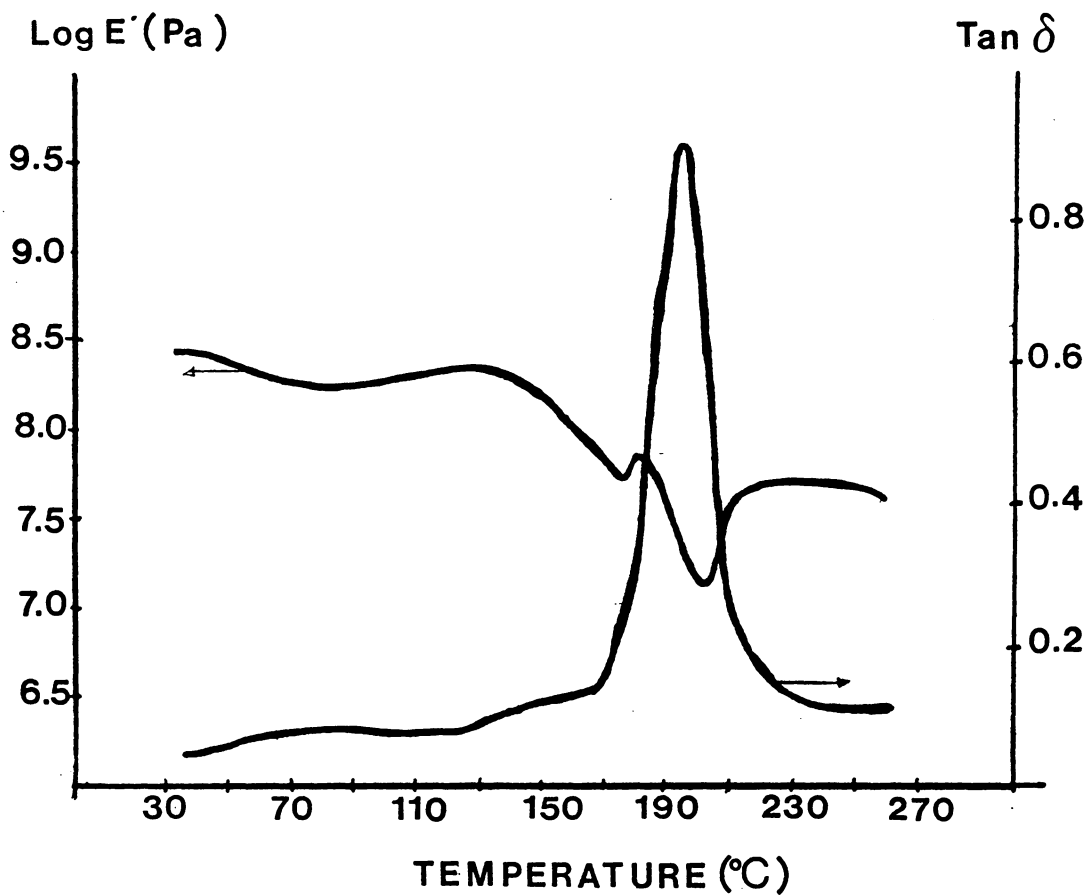


Figure 12: DMTA curve of Parent CTA (DP = 355).

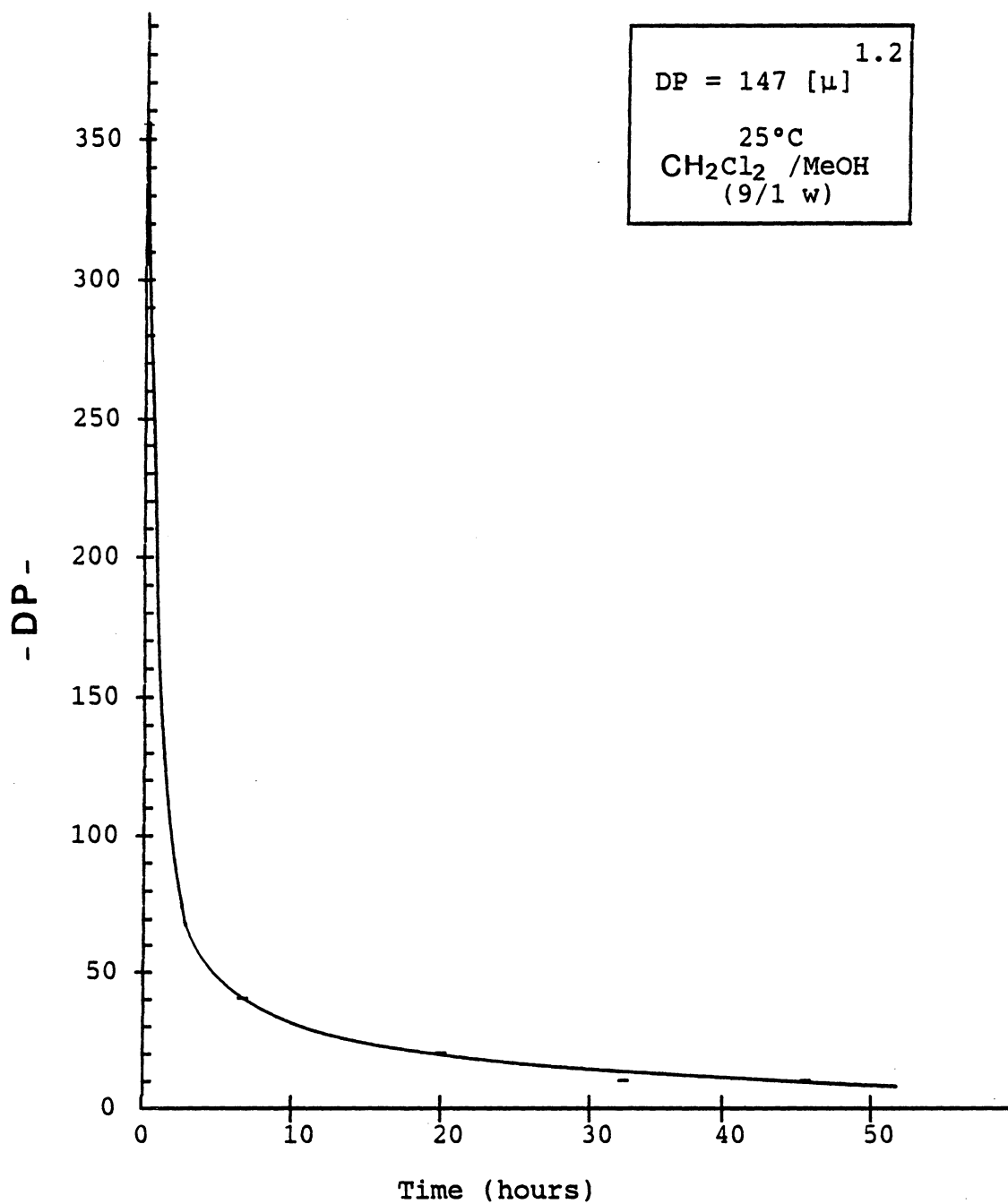


Figure 13: Relationship between degree of polymerization (DP) and time of depolymerization of Parent CTA.

nOH groups/mole

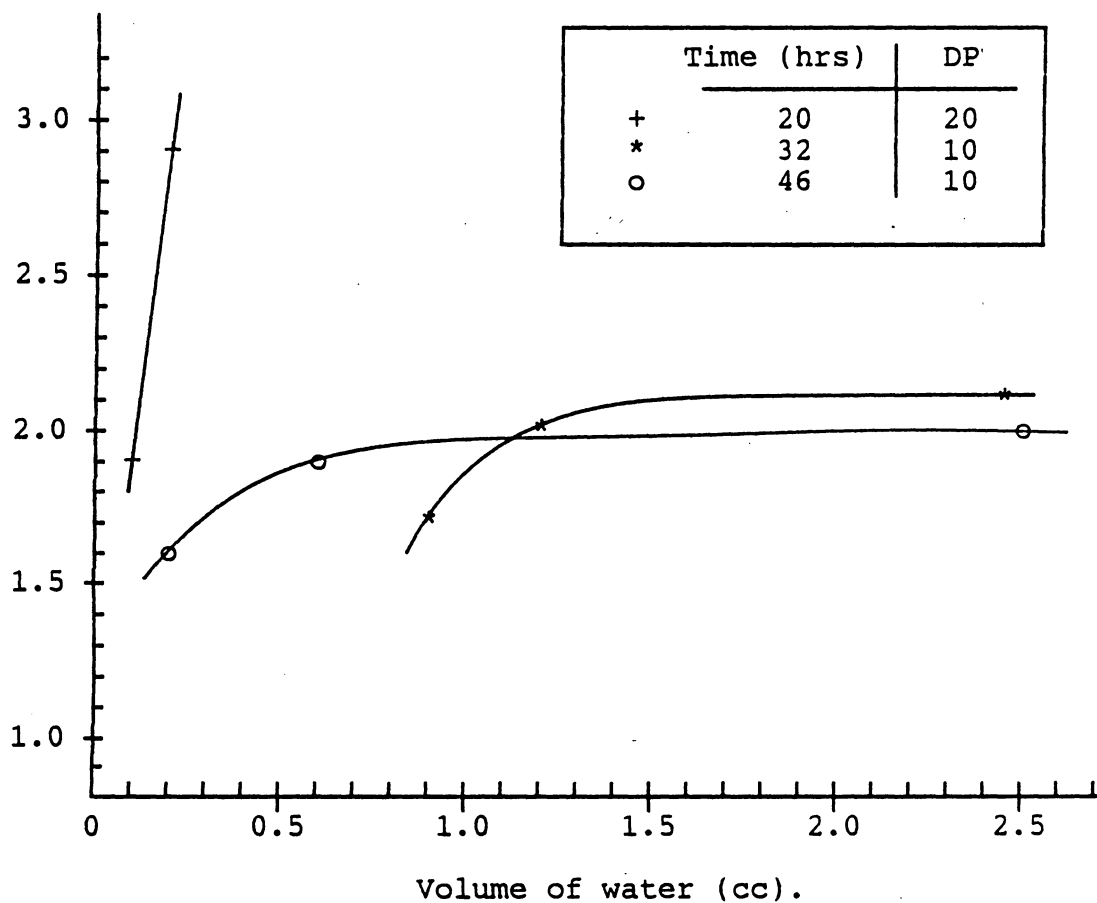


Figure 14: Relation between the hydroxyl functionality of CTA oligomers and the water added at the end of the depolymerization reaction of CTA (DP=355).

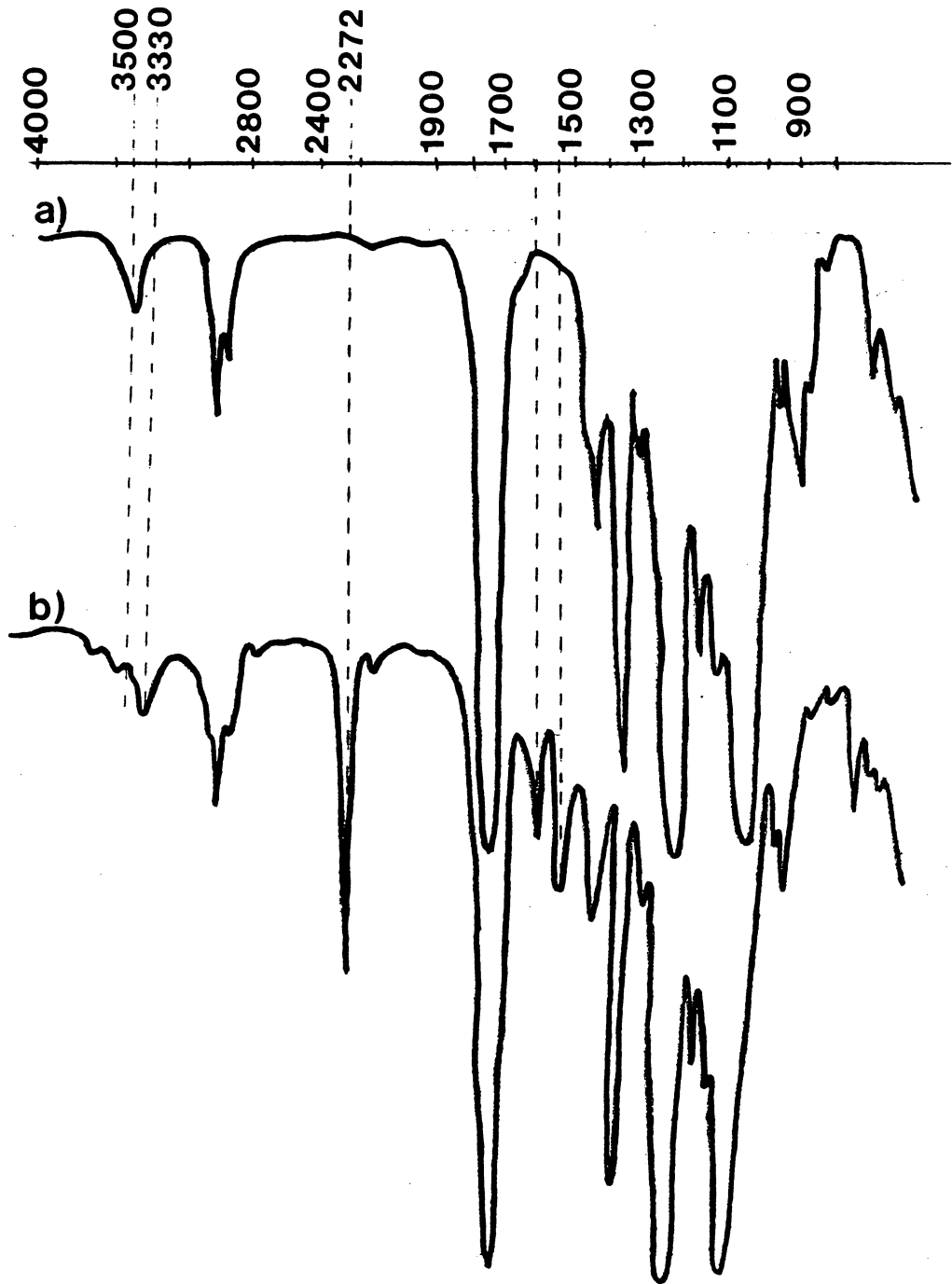


Figure 15: Infrared spectrum of:
a) CTA-oligomer of DP=20 (C20).
b) TDI capped oligomer C20 (TC20).

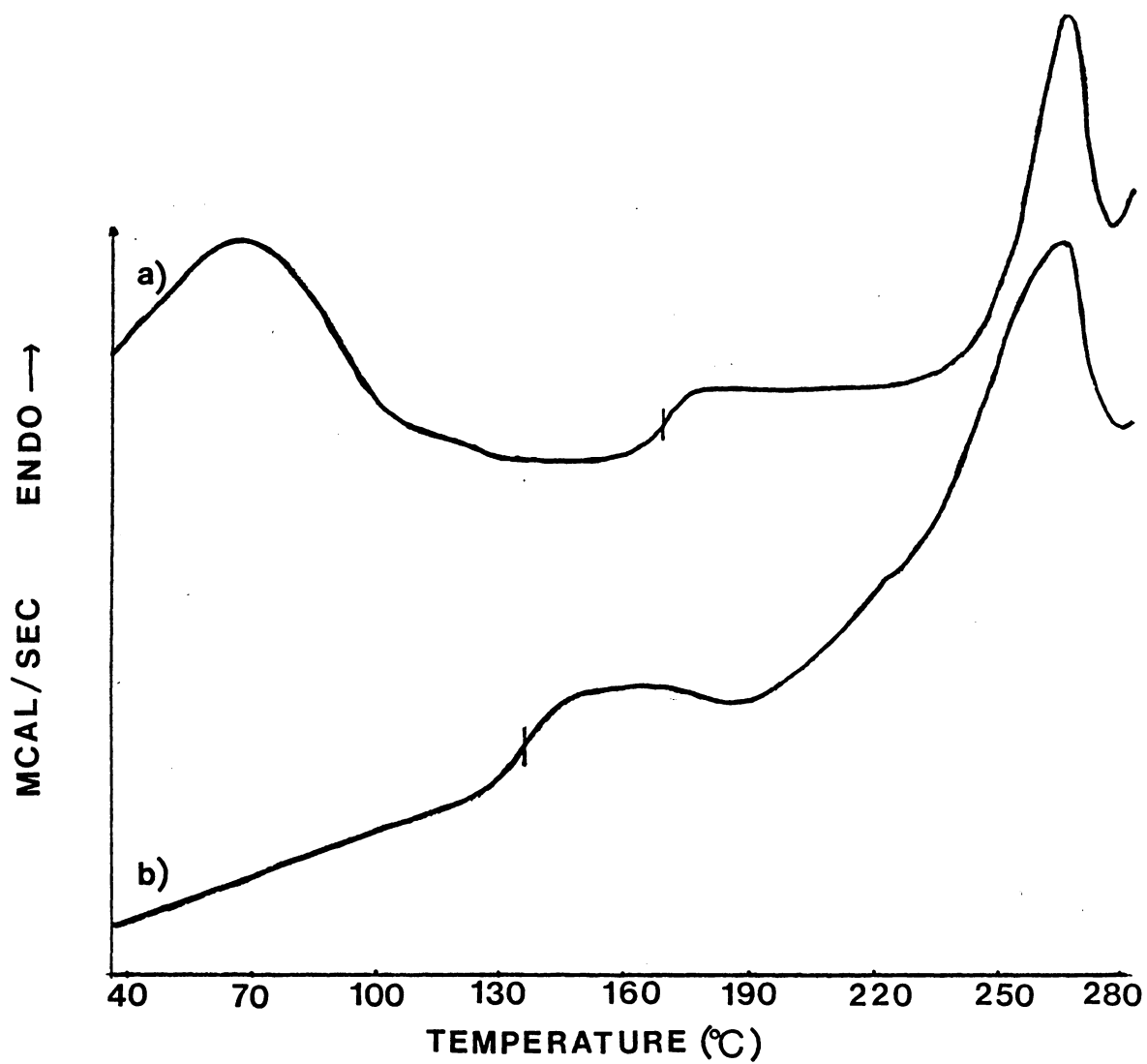


Figure 16: DSC thermogram of:
a) TDI capped oligomer C20 (TC20).
b) TDI capped oligomer C32 (TC32).

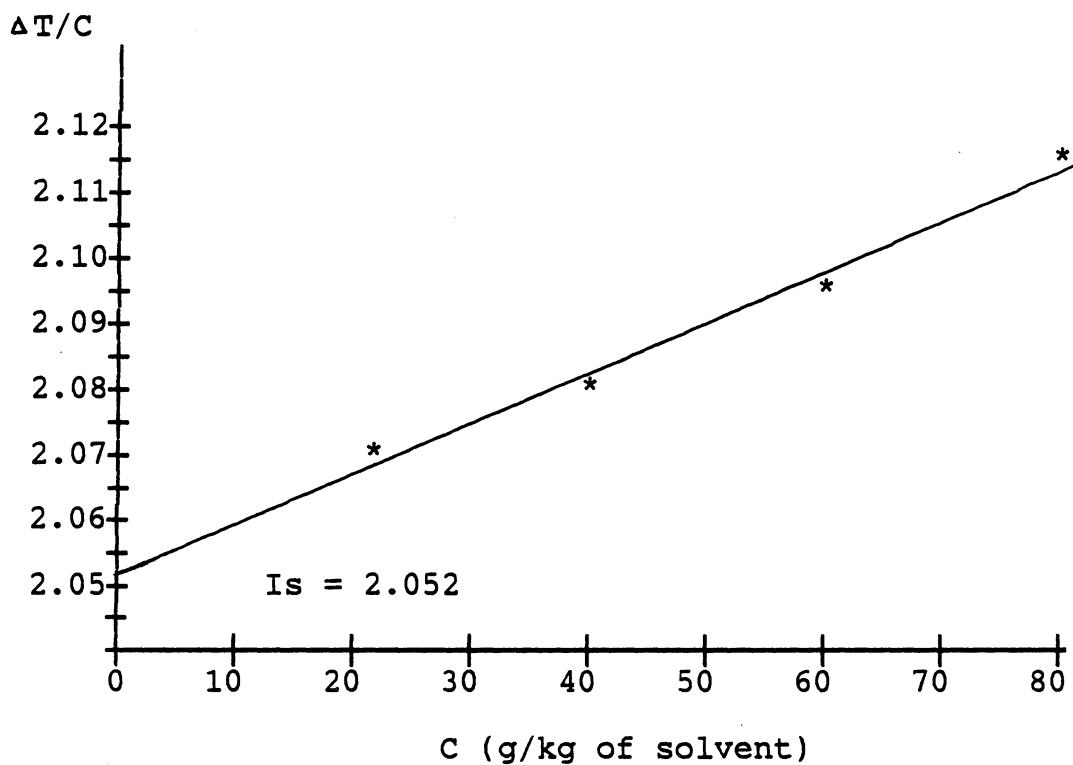


Figure 17: VPO curve for hydroxypropyl lignin (HPL).

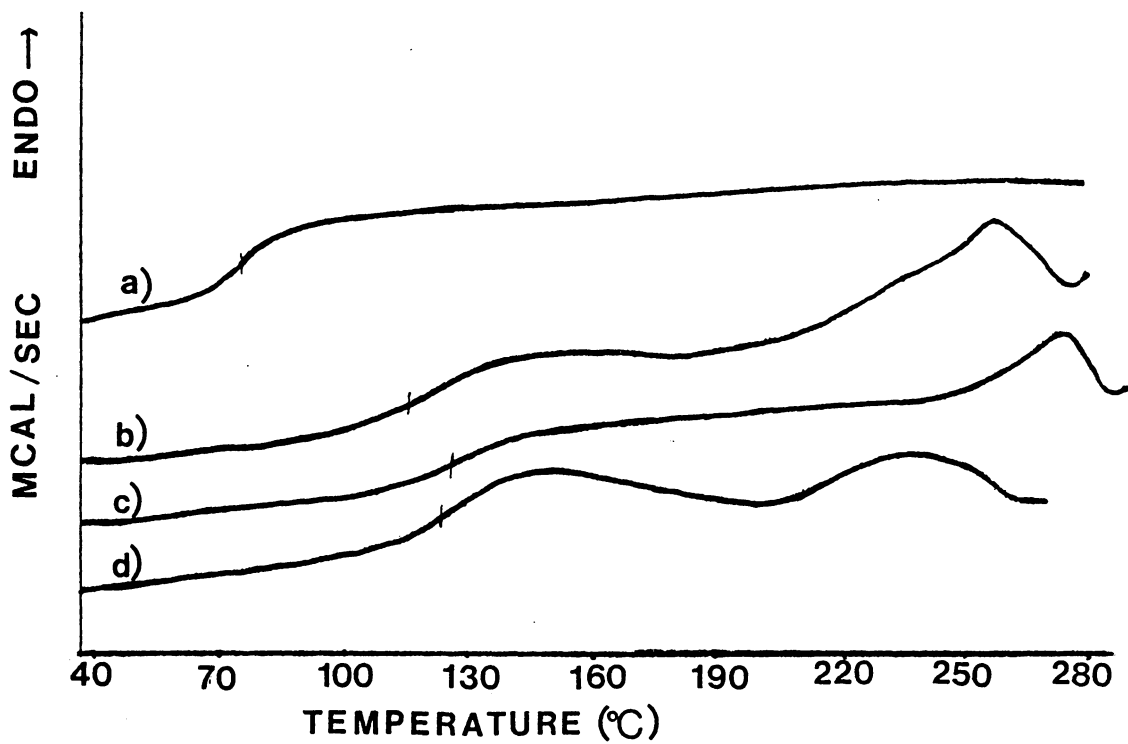


Figure 18: DSC thermogram of: a) hydroxypropyl lignin (HPL)
b) P4608 (copolymer from TC46)
c) P2008 (copolymer from TC20)
d) P3210 (copolymer from TC32)

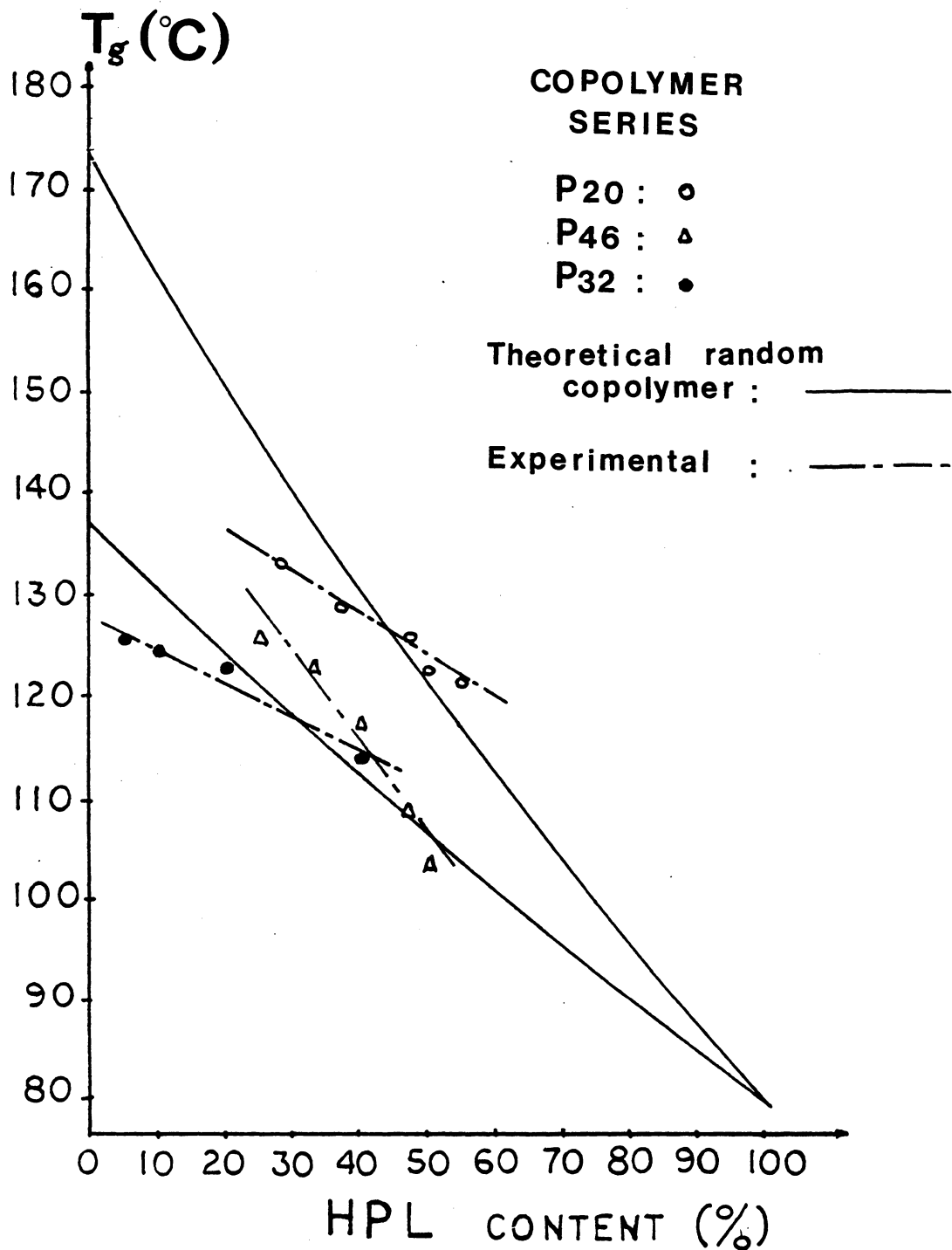


Figure 19: Relationship between HPL content and T_g .

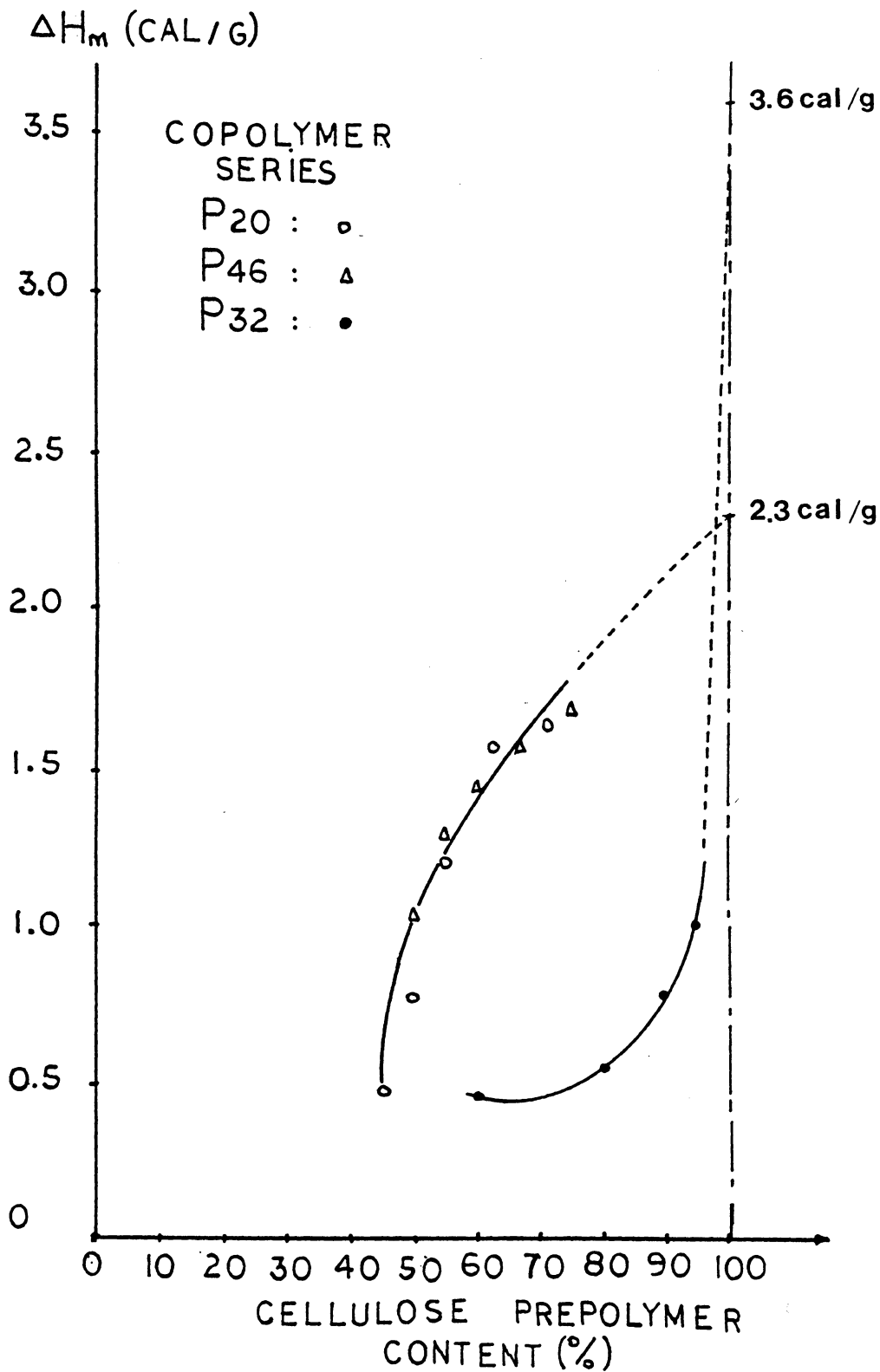


Figure 20: Relationship between heat of fusion, ΔH_m and cellulose content.

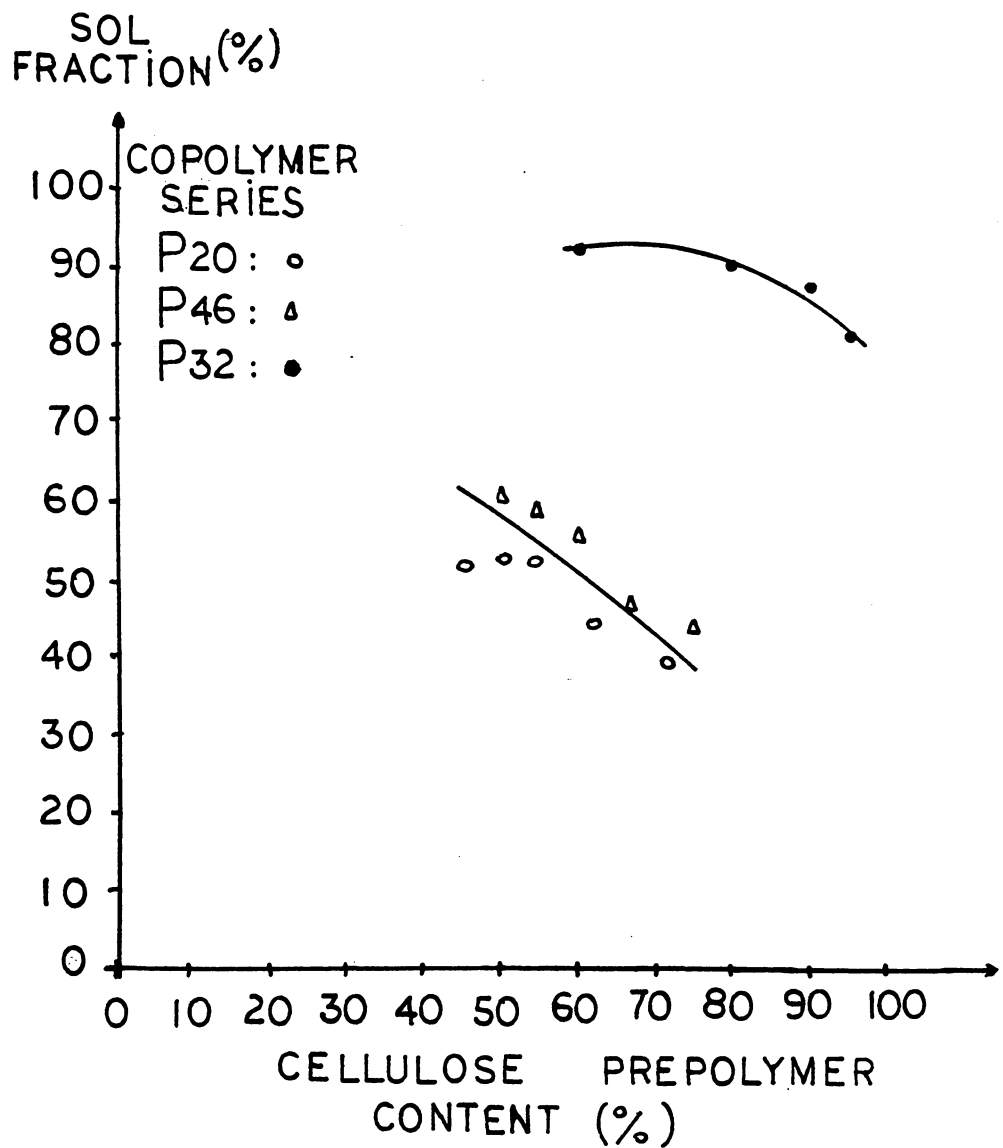
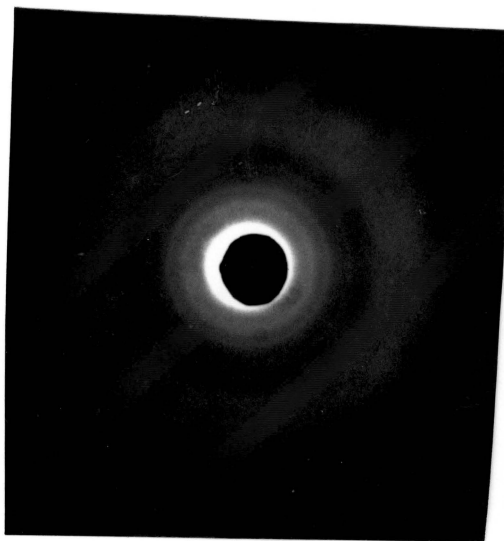
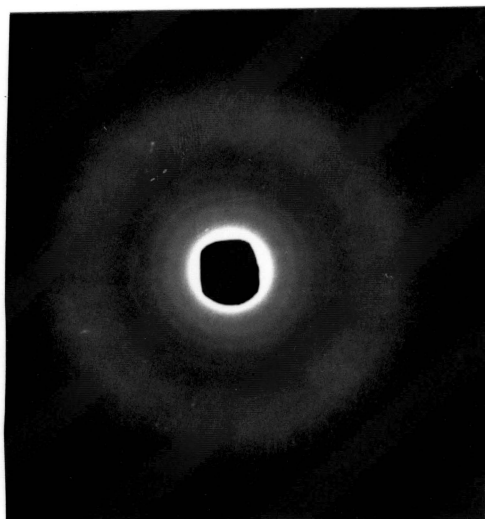


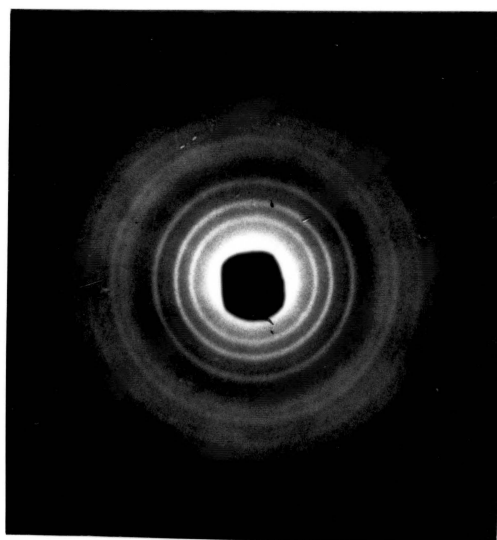
Figure 21: Relationship between sol fraction and polysaccharide block content .



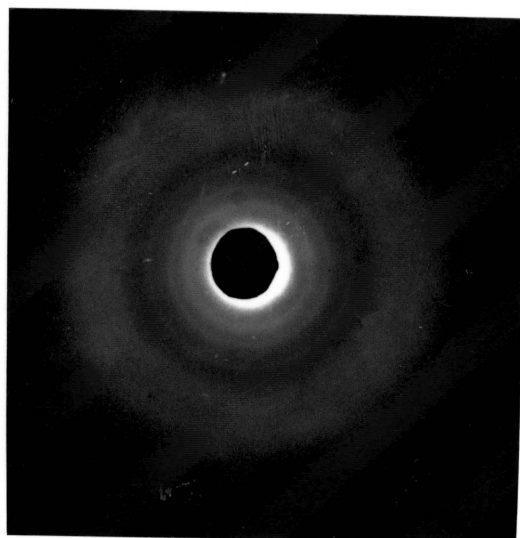
(a)



(b)



(c)



(d)

Figure 22: WAXS results: (a) P3220 ; (b) P3240 ;
(c) P4604 ; (d) P4608.

Table I- Characteristics of CTA block component.

Structural Features	Time of depolymerization (hours)			
	46	32	20	5
<u>CTA oligomers</u>				
Identification number	C46	C32	C20	C5
\bar{M}_n	3015	2631	5814	12500
DP	10-11	10	20	45
nOH/mole	1.9	1.9	2.9	9
OH (%)	1.05	1.23	0.95	1.34
<u>TDI capped CTA oligomers *</u>				
Identification number	TC46	TC32	TC20	not soluble
\bar{M}_n	6460	3582	5450	
DP	20	12	20	
NCO (%)	1.27	1.49	1.72	
nNCO/mole	1.96	0.9	2.2	

* TC46 and TC20 reached at 50°C and 4 hours.
 TC32 reached at 25°C and 2.5 hours.

Table II- Infrared assignment bands of C20 and TC20.

Absorption band (cm ⁻¹)	Oligomer C20	Prepolymer TC20
3500	-OH vibration	
3360		-N-H stretching vibration
3024		-C=C vibration (TDI)
2975	-C-H stretching vibration of -CH ₃ acetyl	
2900	-C-H stretching vibration of >CH ₂ and →CH	
2272		-N-C=O stretching vibration
1750	-C=O stretching vibration	
1600-1650		-C=C vibration (TDI)
1540-1550		-N-H bending vibration
1430	-C-H bending vibration of >CH ₂ and →CH	
1390	-C-H bending vibration of -CH ₃ acetyl	
1230 1050	-C-O-C- stretching vibration (glucose unit)	

Table III- DSC results of prepolymers.

Name	T_g ($^{\circ}\text{C}$)	T_m ($^{\circ}\text{C}$)	ΔH_m (cal/g)
TC32 (DP=12)	136.63	263.51	3.54
TC20 (DP=20)	173.31	274.25	2.3
TC46 (DP=20)	174	274.15	2.4
CTA (DP=355)	183.8	296.15	5.6

Table IV - Formulation parameters of the copolymers.

Copolymer Specimen	HPL content (%)	Molar OH/NCO ratio
1)		
Series P46 -----		
P4612	50	12
P4610	45.5	10
P4608	40	8
P4606	33.3	6
P4604	25	4
2)		
Series P20 -----		
P2012	55	12
P2010	50	10
P2008	45.5	8
P2006	37.6	6
P2004	28.7	4
3)		
Series P32 -----		
P3240	40	6.7
P3220	20	2.5
P3210	10	1
P3205	5	0.5

- 1) From TC46 (the last two digits indicate the OH/NCO ratio)
- 2) From TC20 (the last two digits indicate the OH/NCO ratio)
- 3) From TC32 (the last two digits indicate the HPL content).

Table V- Thermal characteristics from DSC experiments.

Copolymer Specimen	HPL content (%)	T _g (°C) experimental	T _m (°C)	ΔH _m (cal/g)	T _g (°C) * theoretical
Series P46					
P4612	50	103.56	258.11	1.03	
P4610	45.5	109.72	257.93	1.28	
P4608	40	116.97	255.03	1.44	
P4606	33.3	123.38	257.69	1.57	
P4604	25	126.21	254.32	1.68	
Series P20					
P2012	55	121.67	282.44	0.47	116.94
P2010	50	121.71	273.41	0.79	121.40
P2008	45.5	127.32	273.96	1.20	125.66
P2006	37.6	128.34	274.41	1.57	133.00
P2004	28.7	132.50	258.32	1.62	142.00
Series P32					
P3240	40	112.86	251.92	0.47	112.14
P3220	20	122.67	250.35	0.54	124.00
P3210	10	124.62	239.54	0.77	130.05
P3205	5	125.77	246.42	0.99	133.40

* Theoretical values calculated from the model by Fox, (Eq.12)

Table VI- Results from the swelling studies.

Copolymer Sample	cellulose content (%) *	SW (%)	sol fraction (%)
Series P46			

P4612	50	929.20	61.30
P4610	54.6	950.90	59.30
P4608	60	851.87	55.74
P4606	67	715.50	47.60
P4604	75	662.91	43.45
Series P20			

P2012	45	700.00	51.40
P2010	50	724.00	54.70
P2008	54.5	600.00	54.70
P2006	62.4	516.00	44.60
P2004	71.3	396.00	40.00
Series P32			

P3240	60	391.50	93.00
P3220	80	150.00	91.50
P3210	90	62.40	88.50
P3205	95	21.70	81.70

* TC32 content (%) for P32 series
 TC20 content (%) for P20 series
 TC46 content (%) for P46 series

Appendix I

Summary of the analytical results obtained on the Parent cellulose triacetate (CTA) and HPL.

CTA

$$\bar{M}_n = 99258 \text{ g/mole}$$

$$M_u = 279.6 \text{ g/mole}$$

$$DP = 355$$

$$\text{nOH/ unit glucose} = 0.14$$

$$\text{nOH/ mole of CTA} = 50$$

$$\text{nOAc/ unit glucose} = 2.8$$

$$[\mu] = 2.086 \text{ dl/g}$$

$$\%OH = 0.855$$

$$\%OAc = 43.17$$

$$T_g = \text{Glass transition temp.} = 183.8^\circ\text{C}$$

$$T_m = \text{Melting point} = 296.15^\circ\text{C}$$

HPL

$$\bar{M}_n = 2615 \text{ g/mole}$$

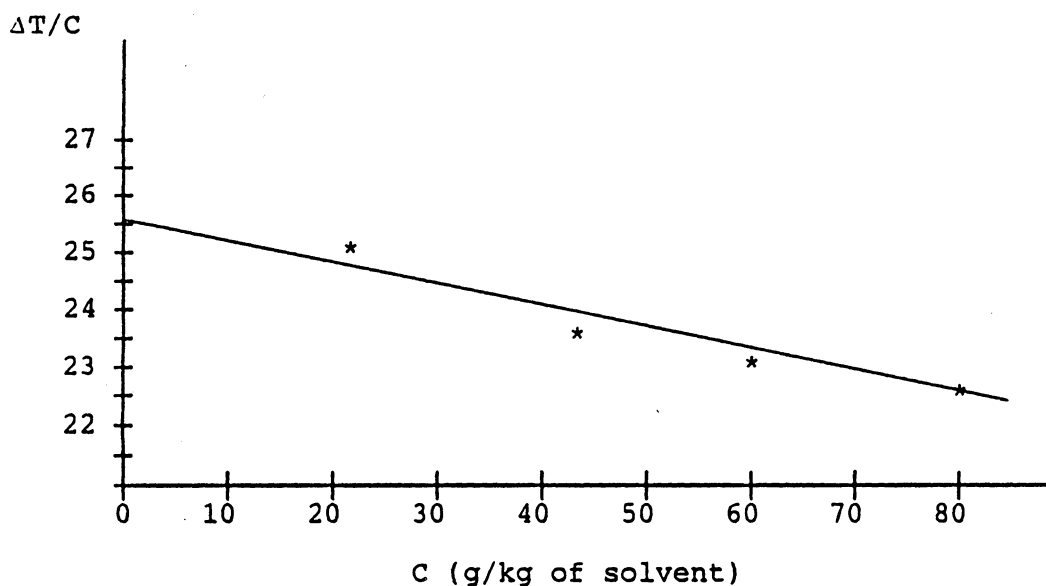
$$\%OH = 6.06$$

$$T_g = 80.3^\circ\text{C}$$

Appendix II

When using the vapor pressure osmometry technique, a reference curve must be obtained. To do that, the reference compound, Benzil of known molecular weight ($M=210.22$ g/mole) was chosen. Concentration varying from 20 to 80 g/ (kg of solvent) were prepared in ethylene chloride 1-2 and the temperature variation ΔT was measured at 45°C . The linear relation obtained between $\Delta T/C$ and C is shown below. ΔT is the variation of temperature between a benzil solution of known concentration and the pure solvent, and C the concentration of the solution.

The intercept at infinite dilution is calculated by linear regression as $I_b = 25.53$. This permits to calculate the coefficient K as: $K = M \times I_b = 5367.17$.



VPO calibration curve (Benzil).

BIBLIOGRAPHY

1. K. Freudenberg and K. Eugler, *Ber* , 71, 1817 (1938).
2. K. Freudenberg, *Ber* , 73, 167 (1940).
3. K. Freudenberg and A.C. Neish, "Constitution and biosynthesis of lignin", Springer-Verlag , NY (1968).
4. K. Freudenberg, *Science* , 148, 595 (1965).
5. A. Sakakibara, *Wood Science and Technology* , 14(2), 89 (1980).
6. E. Adler, *Wood Science and Technology* , 11(3), 169 (1977).
7. W. G. Glasser and H. R. Glasser, *Macromolecules*, 7, 17 (1974).
8. W. G. Glasser and H. R. Glasser, *Holzforschung* , 28(1), 5 (1974).
9. F. E. Braun, *Tappi* , Monograph. Ser., N° 6, 108, (1948).
10. H. Erdtman, *Tappi* , 32, 71 (1949).
11. E. Alder, *Chem. Eng. News* , 34, 4776, (Oct. 1, 1956).
12. E. Alder, *Ind. Eng. Chem* , 49, 1377 (1957).
13. I. A. Pearl, "The chemistry of Lignin", (1967).
14. R. F. Nichols, US Patent N° 2,854,422 (1958).
15. G. S. Mills and H. E. Haxo, US Patent N° 2,906,718 (1959).
16. K. Kratzl, K. Buchtela, J. Gratzl, J. Zauner, and O. Ettinghansen, *Tappi* , 45(2), 113 (1962).
17. G. G. Allan, US Patent N° 3,476,795 (1969).
18. H. H. Moorer, W. K. Dougherty and F. J. Ball, US Patent N° 3,519,581 (1970).
19. T. R. Santelli and R. T. Wallace, US Patent N° 3,577,358 (1971).

20. G. G. Allan, "Occurrence, formation, structure and reaction in lignins", K.V.Sarkanen, C.H Ludwig, Eds. Wiley Intersciences, p 511, (1971).
21. W. G. Glasser and O.H.-H. Hsu, US Patent N^o 4,017,474, (1977).
22. H. Ishikawa and R. Senzyn, *J. Agr. Chem. Soc. Jpn.* , 22,72 (1948).
23. C. F. Wu, MS Thesis "Hydroxypropylation of lignin and lignin-like model compounds", Blacksburg VPI & SU (1982).
24. V. P. Saraf and W. G. Glasser, *J. of App. Polym. Sci.* , Vol. 29, 1831-41, (1984).
25. V. P. Saraf, W. G. Glasser, G. L. Wilkes, and J. E. McGrath, *J. of App. Polym. Sci.* , Vol 30, 2207-24, (1985).
26. V. P. Saraf, W. G. Glasser and G. L. Wilkes, *J. of App. Polym. Sci.* , Vol 30, 3809-23 (1985).
27. T. G. Rials and W.G. Glasser, *Holzforchung* , 38, 263-69, (1984).
28. J. F. Kennedy and G. O. Phillips, "Cellulose & its derivatives, Chem. Biochem. & Applications", (1985).
29. T. P. Nevell and S. H. Zeronian, "Cellulose Chem. & its Applications", (1985).
30. R. M. Rowell and R. A. Young, "Modified Cellulosics" Academic press (1978).
31. D. N. S. Hon, "Graft copolymerization of lignocellulosic Fibers " , Am. Chem. Soc. Washington, D.C (1982).
32. L. J. Tanghe, L. B. Genung and J. W. Mench, *Methods in Carbohydrate Chem.* , Vol.3, p 193-98, (1963), Whisler Ed., Interscience N.Y .
33. B. S. Sprague and L. I. Horner, *Encyclopedia of Polym. Sci. and Tech.* , Vol.3, pp 419-54, N.M. Bikales Ed., Interscience NY, (1965).
34. S. Kim, V. T. Stannett and R. D. Gilbert, *Journal of Polymer Sciences-Polymer Letters Edition* , Vol 11, pp 731-35 (1973).
35. B. G. Penn, V. T. Stannett and R. D. Gilbert, *Macrocromol. Sci.-Chem* , A16(2), 473-79, (1981).
36. S. Kim, V. T. Stannett, and R. D. Gilbert *J. Macromol. Sci. - Chem* , A10 (4), pp 671-79, (1976).
37. R. Amick, V. T. Stannett, and R. D. Gilbert, *Polymer* , Vol. 21, June (1980).
38. M. M. Lynn, V. T. Stannett, and R. D. Gilbert, *J. of Polym. Sci.- Polym. Chem. Ed.* , Vol. 18, pp 1967-1977 (1980).

39. M. M. Lynn, V. T. Stannett and R. D. Gilbert, *Polym. Prep. Am. Chem. Soc. Div. Polym. Chem* , 19(2), pp 106-110 (1978).
40. K. S. Lee, V. T. Stannett, and R. D. Gilbert, *J. Polym. Sci.-Polym. Chem. Ed* , Vol. 20, 997-1009 (1982).
41. H. W. Steinmann, *Polym. Prep.* , Vol. 11(1), 285,(1970).
42. L. Pohjola, O. Harva, and J. Karvinen, *Finn. Chem. Lett.* , 1974, 221-224 (1974).
43. L. Pohjola and V. Eklund, *Paperi Ja Puu* , N°3, pp 117-20, (1977).
44. T. Mezger, H. J. Cantow, *Polym. Photochemistry* , 49-56 (1984).
45. K. Kurita, N. Hirakawa and Y. Iwakura, *Makromol. Chem* , 180, 855-858 (1979).
46. C. Feger and H. J. Cantow, *Polym. Bull.* , 3, 407-413, (1980).
47. D. C. Allport and W. H. Janes, "Block Copolymers", Appl. Sci. Pub. LTD London (1973).
48. J. E. McGrath, *J. of Chem. Education* , Vol. 58, Page 914, (1981).
49. S. S. Kelley, PhD dissertation, V.P.I. and S.U., Blaskburg, Virginia (1986).
50. N. D. Ghatge, M. B. Sabne, S. S. Mahajan and, K. B. Gujar, *J. of Appl. Polym. Sci.* , Vol. 29, 1743-1748, (1984).
51. R. Rahman and Y. Avny, *J. of Macromol. Sci. Chem.* , A12 (8), 1109-1116, (1978).
52. Rahman R., Avny Y., *J. of Macromol. Sci. Chem.* , A13 (7), 953-969, (1979).
53. J. H. Saunders and K. C. Frish, *High Polymers* , Vol. XVI, "Polyurethanes Chemistry and Technology ", 1962 , Wiley Intersc. Publ.
54. G. Lunardon, Y. Sumida and O. Volg , *Angew. Makromol. Chem* , 87, 1, (1980).
55. L.C.-F. Wu and W. G. Glasser, *J. of App. Polym. Sci.* , Vol.29, 1111-1123, (1984).
56. W. G. Glasser, C. A. Barnett, T. G. Rials and, V. P. Saraf, *J. of Polym. Scie.* , Vol.29, 1815-30 (1984).
57. L. J. Tanghe, L. B. Genung and, J. W. Mench, *Methods in carbohydrate chemistry* , Vol. 3, (32), p 201-203 (1963), Whisley Ed., Intersc. N.Y.

58. C. J. Malm, L. J. Tanghe, B. C. Laird, and G. D. Smith, *Anal. Chem.* , Vol. 26, N^o1, (January 1954).
59. L. J. Tanghe, L. B. Genung and J. W. Mench, *Methods in carbohydrate chemistry* , Vol. 3, (33), p 203-207, (1963), Whisler Ed., Intersc. N. Y.
60. L. J. Tanghe, L. B. Genung and J. W. Mench, *Methods in carbohydrate chemistry* , Vol. 3, (35), p 210-12 (1963), Whisler Ed., Intersc. N. Y.
61. W. R. Sorenson and T. W. Campbell, " Preparative methods of polymer chemistry " , p 138, (1961), Intersc. Pub. Inc., N. Y.
62. J. N. Suthar, M. J. Patel, K. C. Patel and, R. D. Patel, *Die. Angrew. Makromol. Chem.* ,130, 125-136, (1985) (Nr.2068).
63. J. M. Cowie and R.J. Ranson, *Die Makromolekulare Chemie* , 143, 105-114, (1971) (Nr.3516).
64. T. G. Fox, *Bull. Amer. Phys. Soc.* , 1, 123 (1956).
65. M. Droscher, *Makromol. Chem. Suppl.* , 6, 107-116, (1984).
66. G. L. Clark, *Ind. Eng. Chem.* , 22(10), N^o5, 474 (1930).
67. G. L. Clark, "The encyclopedia of X-rays and Gamma rays", p 866 (1963), Reinhold Publishing Corporation.
68. G. L. Clark, "Applied X-rays", (1927), McGraw Hill Book Company, Inc. ,N.Y.
69. W. O. Baker, C. S. Fuller and, N. R. Pape, *J. of Am. Chem. Soc.* , Vol. 64, 776-782, (1942).
70. A. J. Stamm, " Wood and Cellulose Science", Chap.2, (1964), Ronald Press Company.
71. I. Slowikowska, and I. Daniewska , *J. Polym. Sci.* , 53, 187-93, (1975).
72. M. Gervais and B. Gallot, *Makromol. Chem.* , 178, 1577-93, (1977).

**The vita has been removed from
the scanned document**